

Manuscript Details

Manuscript number	MARMIC_2019_30_R2
Title	Distribution of common modern dinoflagellate cyst taxa in surface sediments of the Northern Hemisphere in relation to environmental parameters: the new n = 1968 database
Article type	Research Paper

Abstract

We present a new version of the standardized Northern Hemisphere “modern” dinoflagellate cyst (“dinocyst”) database, which includes abundances of 71 taxa at 1968 sites across the Northern Hemisphere, cross-referenced with 17 environmental parameters extracted mostly from the 2013 World Ocean Atlas. Several taxa with tropical to warm temperate affinities were added to the previous database version. Dinocyst concentrations in the surface sediments reach 106 cysts g⁻¹, with maximum values along the continental margins and minimum values offshore in distal open ocean settings. The assemblages are characterized by the co-occurrence of phototrophic (n=41) and heterotrophic taxa (n=30), with maximum proportions of heterotrophic taxa in high productivity regions, notably at the sea-ice edge and in upwelling regions. The main pattern of the assemblage distribution includes north–south and nearshore–offshore gradients, with maximum diversity of species along the continental margins and towards the south, in warm temperate and tropical areas. Canonical correspondence analyses performed on heterotrophic and phototrophic taxa independently yield consistent results, hence suggesting similar, but not identical, ecological affinities for both taxonomic groups. For both groups, sea-surface temperature and sea-ice are the most determining parameters, but the phototrophic taxa seem more sensitive to onshore–offshore gradients marked by salinity changes. Productivity-related parameters are also a determinant of dinocyst distribution, especially primary productivity in the fall and winter, with a stronger relationship for the combined dataset of phototrophic and heterotrophic taxa.

Keywords	dinocysts; North Atlantic, Arctic, North Pacific; oceanography; productivity;
Manuscript region of origin	North America
Corresponding Author	Anne de Vernal
Corresponding Author's Institution	GEOTOP-UQAM
Order of Authors	Anne de Vernal, Taoufik Radi, Sébastien zaragosi, Nicolas Van Nieuwenhove, Andre Rochon, Estelle Allan, Stijn De Schepper, Frederique Eynaud, Martin Head, Audrey Limoges, Laurent Londeix, Fabienne Marret-Davies, Jens Matthiessen, Vera Pospelova, Andrea Price, Thomas Richerol
Suggested reviewers	Sophie Warny, Marit-Solveig Seidenkrantz, John Williams, Appy Sluijs

Submission Files Included in this PDF

File Name [File Type]

Letter to Editor-revised-AdV et al-BD1968-R2.pdf [Cover Letter]

response to reviewers.docx [Response to Reviewers]

BD1968-Highlight.docx [Highlights]

R2-abstract.docx [Abstract]

R2-txt-BD1968-2nov.docx [Manuscript File]

R2-Figure 1.pdf [Figure]

R2-Figure 2.pdf [Figure]

R2-Figure 3.pdf [Figure]

R2-Figure 4.pdf [Figure]

R2-Figure 5a-d.pdf [Figure]

R2-Figure 5-e-h.pdf [Figure]

R2-Figure 5-i-l.pdf [Figure]

R2-Figure 5m-p.pdf [Figure]

R2-Figure 5q-t.pdf [Figure]

R2-Figure 5u-x.pdf [Figure]

R2-Figure 5-y.pdf [Figure]

R2-Figure 6.pdf [Figure]

R2-Figure 7.pdf [Figure]

R2-Figure 8.pdf [Figure]

R2-Figure S1a.pdf [Figure]

R2-Figure S1b.pdf [Figure]

R2-Figure S1c.pdf [Figure]

declaration-of-competing-interests-AdV.pdf [Manuscript File]

Submission Files Not Included in this PDF

File Name [File Type]

R2-TABLE 1.xlsx [Table]

R2-TABLE 2.xlsx [Table]

R2-TABLE 3.xlsx [Table]

R2-TABLE 4a.xlsx [Table]

R2-TABLE 4b.xlsx [Table]

R2-TABLE 4c.xlsx [Table]

R2-TABLE 5.xlsx [Table]

R2-Table S1.xlsx [Table]

R2-Table S2.xlsx [Table]

R2-Table S3a.xlsx [Table]

R2-Table S3b.xlsx [Table]

R2-Table S3c.xlsx [Table]

R2-Table S4a.xlsx [Table]

R2-Table S4b.xlsx [Table]

R2-Table S4c.xlsx [Table]

To view all the submission files, including those not included in the PDF, click on the manuscript title on your EVISE Homepage, then click 'Download zip file'.

Research Data Related to this Submission

There are no linked research data sets for this submission. The following reason is given:

All data are included in Table or as supplementary material. The main data (Table s2) were also submitted to Pangaea.



November 2, 2019

Dr. Richard Jordan
Editor in Chief, *Marine Micropaleontology*

Dear Dr. Jordan,

Please find attached the second revised version of the manuscript now entitled “Distribution of common modern dinoflagellate cyst taxa in surface sediments of the Northern Hemisphere in relation to environmental parameters: the new n = 1968 database”.

The main changes in the text, tables and figures concern the updating of the nomenclature for consistency with the manuscripts by Van Nieuwenhove et al., Mertens et al., Limoges et al., and Head et al. (same issue).

Another change concern the explanation about the calculation of the distance, which now reads as follows (page 13) “The distance to the coast is expressed in km. It was calculated with ARCGIS using geodetic distances between features. The method based on the World Geodetic System (WGS 84; <https://gisgeography.com/wgs84-world-geodetic-system/>), which takes into account the curvature of the spheroid and correctly deals with data near the dateline and poles.” Thanks to the comments by the reviewer, we have made tests to evaluate what is the most accurate method and we recalculated the distance and performed again the CCA analyses (figure 6 modified slightly). All tables now refer to the correct distances.

I have edited the text as suggested by you and reviewer #1 (thank you !). and the text was proof-read by Martin Head. The tables and figures were also verified. The data were submitted to Pangaea for archiving (<https://issues.pangaea.de/browse/PDI-22046>).

I hope that the manuscript is now suitable for publication. I thank you very much for your attention.

Best regards,

Anne de Vernal

Response to comments by editor and reviewers.

As indicated in the cover letter, the main changes in the text, tables and figures concern the updating of the nomenclature for consistency with the manuscripts by Van Nieuwenhove et al., Mertens et al., Limoges et al., and Head et al. (same issue).

Another change concern the explanation about the calculation of the distance, which now reads as follows (page 13) “The distance to the coast is expressed in km. It was calculated with ARCGIS using geodetic distances between features. The method based on the World Geodetic System (WGS 84; <https://gisgeography.com/wgs84-world-geodetic-system/>), which takes into account the curvature of the spheroid and correctly deals with data near the dateline and poles.” Thanks to the comments by the reviewer, we have made tests to evaluate what is the most accurate method and we recalculated the distance and performed again the CCA analyses (figure 6 modified slightly). All tables now refer to the correct distances.

The text has been edited as suggested by the editor and reviewer #1. Moreover, the text was proof-read by Martin Head. The tables and figures were also verified.

The data were submitted to Pangaea for archiving (<https://issues.pangaea.de/browse/PDI-22046>).

“Distribution of common modern dinocyst taxa in surface sediments of the Northern Hemisphere in relation to environmental parameters: the updated n=1968 database”,

Highlights :

- Exhaustive dinocyst assemblage data (71 taxa) from 1968 samples are presented
- Relationship with 17 environmental parameters are explored
- Dinocyst assemblages are closely related to salinity, temperature, sea-ice cover and productivity
- The database permits to disentangle salinity from temperature

We present a new version of the standardized Northern Hemisphere “modern” dinoflagellate cyst (“dinocyst”) database, which includes abundances of 71 taxa at 1968 sites across the Northern Hemisphere, cross-referenced with 17 environmental parameters extracted mostly from the 2013 World Ocean Atlas. Several taxa with tropical to warm temperate affinities were added to the previous database version. Dinocyst concentrations in the surface sediments reach 10^6 cysts g^{-1} , with maximum values along the continental margins and minimum values offshore in distal open ocean settings. The assemblages are characterized by the co-occurrence of phototrophic (n=41) and heterotrophic taxa (n=30), with maximum proportions of heterotrophic taxa in high productivity regions, notably at the sea-ice edge and in upwelling regions. The main pattern of the assemblage distribution includes north–south and nearshore–offshore gradients, with maximum diversity of species along the continental margins and towards the south, in warm temperate and tropical areas. Canonical correspondence analyses performed on heterotrophic and phototrophic taxa independently yield consistent results, hence suggesting similar, but not identical, ecological affinities for both taxonomic groups. For both groups, sea-surface temperature and sea-ice are the most determining parameters, but the phototrophic taxa seem more sensitive to onshore–offshore gradients marked by salinity changes. Productivity-related parameters are also a determinant of dinocyst distribution, especially primary productivity in the fall and winter, with a stronger relationship for the combined dataset of phototrophic and heterotrophic taxa.

Distribution of common modern dinoflagellate cyst taxa in surface sediments of the Northern Hemisphere in relation to environmental parameters: the new n = 1968 database

Anne de Vernal¹, Taoufik Radi¹, Sebastien Zaragosi², Nicolas Van Nieuwenhove³, André Rochon⁴, Estelle Allan¹, Stijn De Schepper⁵, Frédérique Eynaud², Martin J. Head⁶, Audrey Limoges³, Laurent Londeix², Fabienne Marret⁷, Jens Matthiessen⁸, Aurélie Penaud⁹, Vera Pospelova¹⁰, Andrea Price^{12,13}, Thomas Richerol⁴

¹ Geotop, Université du Québec à Montréal (UQAM), 201 Avenue du Président Kennedy, Montréal, Québec, H3C 3P8, Canada

² Université de Bordeaux, UMR CNRS 5805 EPOC (Environnements et Paléoenvironnements Océaniques et Continentaux), Allée Geoffroy St Hilaire, 33615 Pessac Cedex, France

³ Department of Earth Sciences, University of New Brunswick, 2 Bailey Drive, Fredericton, New Brunswick, E3B 5A3, Canada

⁴ Institut des sciences de la mer de Rimouski, Université du Québec à Rimouski, 310 Allée des Ursulines, Rimouski, Québec, G5L 3A1, Canada

⁵ NORCE Norwegian Research Centre, Bjerknes Centre for Climate Research, Jahnebakken 5, 5007 Bergen, Norway

⁶ Department of Earth Sciences, Brock University, 1812 Sir Isaac Brock Way, St. Catharines, Ontario, L2S 3A1, Canada

⁷ Department of Geography and Planning, School of Environmental Sciences, University of Liverpool, L69 7ZT Liverpool, UK

⁸ Alfred Wegener Institute Helmholtz Centre for Polar and Marine Research, Am AltenHafen 26, D-27568 Bremerhaven, Germany

⁹ UMR 6538 Géosciences Océan, IUEM, Université Brest, CNRS, 29280 Plouzané, France

¹⁰ School of Earth and Ocean Sciences, Bob Wright Centre A405, University of Victoria, PO Box 1700, STN CSC, Victoria, British Columbia V8W 2Y2, Canada

¹¹ Department of Geography, McGill University, 805 Sherbrooke Street West, Montréal, Québec, H3A 0B9, Canada

¹²Louisiana Universities Marine Consortium (LUMCON), 8124 Highway 56, Chauvin,
LA 70344 USA

¹³Department of Marine Geosciences, University of Haifa, 199 Abba Khoushy Ave,
Haifa, 3498838 Israel

Abstract

We present a new version of the standardized Northern Hemisphere “modern” dinoflagellate cyst (“dinocyst”) database, which includes abundances of 71 taxa at 1968 sites across the Northern Hemisphere, cross-referenced with 17 environmental parameters extracted mostly from the 2013 World Ocean Atlas. Several taxa with tropical to warm temperate affinities were added to the previous database version. Dinocyst concentrations in the surface sediments reach 10^6 cysts g^{-1} , with maximum values along the continental margins and minimum values offshore in distal open ocean settings. The assemblages are characterized by the co-occurrence of phototrophic ($n=41$) and heterotrophic taxa ($n=30$), with maximum proportions of heterotrophic taxa in high productivity regions, notably at the sea-ice edge and in upwelling regions. The main pattern of the assemblage distribution includes north–south and nearshore–offshore gradients, with maximum diversity of species along the continental margins and towards the south, in warm temperate and tropical areas. Canonical correspondence analyses performed on heterotrophic and phototrophic taxa independently yield consistent results, hence suggesting similar, but not identical, ecological affinities for both taxonomic groups. For both groups, sea-surface temperature and sea-ice are the most determining parameters, but the phototrophic taxa seem more sensitive to onshore–offshore gradients marked by salinity changes. Productivity-related parameters are also a determinant of dinocyst distribution, especially primary productivity in the fall and winter, with a stronger relationship for the combined dataset of phototrophic and heterotrophic taxa.

1. Introduction

Among palynological microfossils, organic-walled dinoflagellate cysts were acknowledged as biostratigraphical markers (e.g., Traverse, 1988 and references therein) well before being useful paleoceanographical indicators. Because of their abundance, taxonomic diversity, and good preservation in most marine sediments of Jurassic to late Cenozoic ages, dinoflagellate cysts, first known as hystrichospheres, were widely used in marine geology and biostratigraphy. However, until the 1960s their biological affinity remained largely unknown, which was a critical limitation for paleoecological applications. Thanks to early culturing studies (e.g. Braarud, 1945; see Head, 1996), observations of cysts within thecae (e.g., Nordli, 1951; Rossignol, 1964), the detailed taxonomic work of Evitt (1961) and others (e.g., Evitt and Davidson, 1964), and *in vitro* experiments of Wall (1965) and Wall and Dale (1968), it has been possible to shed light on the biological relationships between the living cells of dinoflagellates and their cysts, which are now commonly designated as dinocysts. Studies that followed, including Williams (1971), Wall et al. (1977), Harland (1983), Turon (1984) and Mudie and Short (1985), documented the recent distribution of dinocysts on the sea floor, which demonstrated their relevance as paleoecological and paleoclimatic indicators for late Quaternary paleoceanographic studies.

In the 1970s, dinocysts were still rarely used in paleoceanography, but planktonic foraminifers (e.g., Imbrie and Kipp 1971), coccoliths (e.g., Sach, 1973), radiolarians (e.g., Geitzenauer et al., 1976) and diatoms (e.g., Maynard, 1976; Sancetta, 1977) were routinely used in paleoceanographical studies, including the quantitative reconstructions of past sea-surface temperature (SST). Hence the CLIMAP (1976) surface ocean temperatures during the

last glacial maximum (LGM) were drafted based on marine microfossil assemblages, including planktonic foraminifers, coccoliths, diatoms and radiolarians, but not dinocysts. The CLIMAP (1976) reconstructions of marine conditions at high latitudes of the North Atlantic and adjacent polar and subpolar seas, however, suffered from limited data and the very low species diversity of planktonic foraminifer assemblages (e.g., Bé and Tolderlund, 1971), which makes them unsuitable for transfer functions. Moreover, calcareous and siliceous microfossil assemblages may be biased by dissolution, especially in the Arctic basins such as Baffin Bay (e.g., Aksu, 1983). Hence, the development of a standardized dinocyst database in the late 1980s was motivated by the potential of well-preserved and relatively rich assemblages of organic-walled dinocysts to provide information about sea-surface conditions in high latitude marine settings (e.g., Turon, 1984; Mudie and Short, 1985). The initial dinocyst database of the late 1980s first aimed at complementing the CLIMAP (1976) reconstructions of the LGM in the northern North Atlantic (de Vernal et al., 1993a, 1994). It was later used to draw maps of winter and summer SST and salinity (SSS) in addition to sea-ice cover in the northern North Atlantic as a contribution to the Multiproxy Approach for the Reconstruction of the Glacial Ocean surface (MARGO; Kucera et al., 2005; Waelbroeck et al., 2009). The Northern Hemisphere dinocyst database is now routinely used for reconstructions of sea-surface conditions of glacial and interglacial episodes (e.g., Sundqvist et al., 2014; Datema et al., 2017; Falardeau et al., 2018; Caron et al., 2019).

The dinocyst database was built after agreement about the standardization of protocols for palynological extraction and the use of a common intercalibrated taxonomy (Rochon et al., 1999). Since then, the dinocyst database has been regularly updated, taking advantage of regional studies in the North Pacific (Radi and de Vernal, 2004; Radi et al, 2007; Bonnet et

al., 2012), the Nordic Seas (Rochon et al., 1999; Grøsfjeld and Harland, 2001, 2007; Bonnet et al., 2010), the Canadian Arctic (Richerol et al., 2008), the Barents Sea (Voronina et al. 2001; Solignac et al., 2009), the Laptev Sea (Kunz-Pirrung et al., 2001), northern Baffin Bay (Hamel et al., 2002), the southwest USA and western Mexican margins (Pospelova et al, 2008; Vasquez-Bedoya et al., 2008; Limoges et al., 2010) and the Gulf of Mexico (Limoges et al., 2013).

From multivariate analyses performed on the various updates of the database, it appeared that dinocyst assemblages were not exclusively responding to temperatures but were also affected by salinity, seasonal temperature range, sea-ice cover and productivity. Hence, dinocysts were revealed to be useful paleoenvironmental indicators in transitional environments such as estuaries and coastal regions marked by large seasonal temperature gradients (e.g., de Vernal et al., 2001, 2005) and in Arctic and subarctic seas (e.g., de Vernal et al., 2013a, b). Dinocysts were used to reconstruct surface water density, permitting them to address issues of convection and deep-water formation (Hillaire-Marcel et al., 2001; de Vernal et al., 2002; Van Nieuwenhove et al., 2016). They have helped address issues of eutrophication and upwelling (e.g., Pospelova et al., 2005, 2008; Thibodeau et al., 2006; Radi and de Vernal, 2008; Zonneveld et al., 2013; Price et al., 2018). However, there are caveats related to taphonomic processes as well as analyses and data treatments (e.g., de Vernal and Marret, 2007; Zonneveld et al., 2008; Guiot and de Vernal, 2011).

Here we present an updated standardized dinocyst database, which includes 1968 data points (Figure 1; supplementary Tables S1 and S2). From the prior version that included 1492 sites (de Vernal et al., 2013a), we added data from sites in Baffin Bay, the Labrador Sea, the

Nordic Seas and the Arctic Ocean (see Allan et al., 2018, this issue); we extended the geographic domain to the south along the eastern coast of the USA and the Gulf of Mexico (Limoges et al., 2013; Price et al., 2016, 2017b, 2018) and off the western African margin (Marret et al., 2008). By enlarging the size of the database and extending its geographical domain, we aimed both at improving the inferential power of statistical approaches for paleoceanographical reconstructions and enhancing the ability of dinocysts to resolve issues related to climatic and oceanic changes at low latitudes. However, by enlarging the database, it was necessary to revise the taxonomy and reassess the relationship between assemblages and environmental parameters. The taxonomical basis of the species used here is presented in a companion paper by Van Nieuwenhove et al. (this issue), whereas accessory species whose documented modern occurrence is too low to statistically explore their environmental constraints are presented by Limoges et al. (this issue) and Mertens et al. (this issue). Some issues related to taphonomic processes are addressed in Allan et al. (this issue). Here, we illustrate the main features of the dinocyst assemblage distribution. In the accompanying material, we provide all dinocyst counts as well as the environmental values extracted from data held at the National Ocean and Atmospheric Administration (NOAA), the National Snow and Ice Data Centre (NSIDC) and Moderate resolution imaging spectroradiometer (MODIS) of the National Aeronautics and Space Administration (NASA). Multivariate analyses were conducted to explore the significance, usefulness and limitations of the database and its use for paleoclimatic and paleoceanographic inferences. Further tests with the modern analogue technique and transfer functions were made to evaluate the potential of dinocysts for quantitative paleoceanographic reconstructions. Results are reported by Hohmann et al. (this issue).

2. Methods

2.1. Database assembly and standardization

Standardization of sample processing and taxonomy is a prerequisite for data comparison. This is relatively easy to achieve with a small number of samples and analysts. It is, however, more challenging with a large number of samples and when many laboratories and researchers contribute to the analyses. Moreover, since the late 1980s, the taxonomy of late Quaternary including recent dinocysts has evolved considerably, which may limit the use of older samples in the database.

The “standardized” techniques of preparation have been described in all papers presenting regional data sets and database updates. They basically follow the protocol established by de Vernal in the 1980s and presented in tutorials prepared for student training (de Vernal et al., 2010). The main steps of the sample preparation include measurement of the volume by immersion in a graduate cylinder and/or the dry weight sediment prior to mechanical wet sieving of the size fraction (~10–100 µm) containing dinocysts, and repeated chemical treatments with HCl and HF to dissolve carbonates and silicates. There are variations in the techniques, notably for sieving mesh size and chemical treatment duration, but they avoid oxidation techniques because some dinocyst taxa are sensitive to oxidation (de Vernal et al., 2010). Hence, the preparations involve mostly HCl (10%) and HF (40–52%) treatments and centrifugation before decanting. The treatments are usually made at room temperature, but the use of a hot bath to accelerate the reaction was routine in the past. Although warm HF treatment has not been reported to affect the taxa included in the database, a few species might be altered. This is notably the case for the cysts of *Polarella glacialis* and specimens

referred to as cf. *Biecheleria* sp. (e.g. Heikkilä et al., 2014; Limoges et al., 2018), which may, furthermore, have been overlooked before because of their rarity and small size. The sieving mesh size is usually between 10 and 106 μm because the analyses often aim at counting all palynomorphs including acritarchs and pollen grains. However, some studies used mesh sizes of 15 μm (Price et al., 2016, 2017b, 2018) to remove fine silts and amorphous organic matter, and other studies used a mesh size of 63 μm (Rochon et al., 1999) as an upper limit to remove sand particles. Such mesh sizes should not affect the composition of dinocyst assemblages but should be considered as lower and upper limits in order to recover small cysts such as those of *Pentapharsodinium dalei* (19–36 μm) and large cysts such as *Spiniferites mirabilis* (35–76 μm) or *Tuberculodinium vancampoe* (63–135 μm), to name a few (Van Nieuwenhove et al., this issue).

The dinocyst database presented herein (n=1968) includes assemblages for which at least 60 specimens were counted per sample, with an average of 345 specimens per sample (Table S1).

2.2 The taxa

Since the initial development of the database, new taxa have been described and a few others have had their name and description emended. Table 1 provides a list of the taxa (n=41) referred to in the Rochon et al. (1999) monograph, those of de Vernal et al. (2013) database (n=66), and those of the present database, which includes 71 taxa. The number of taxa has increased mostly because of the enlargement of the geographical domain to the Pacific and low latitudes (Table 1). Among species added are *Bitectatodinium spongium*, *Dalella chathamensis*, *Impagidinium plicatum*, *Operculodinium israelianum*,

Operculodinium giganteum, *Operculodinium longispinigerum*, *Polysphaeridium zoharyi*, *Tectatodinium pellitum* and *Tuberculodinium vancampoe*, which all have a temperate–tropical distribution (e.g., de Vernal and Marret, 2007; Marret et al., 2008; Zonneveld et al., 2013; Limoges et al., 2013).

Some taxa were renamed after taxonomic emendation, revision or description. This is notably the case for *Atlanticodinium striaticonulum* (Head and Mantilla-Duran, this issue), *Echinidinium karaense* (Head et al., 2001), *Islandinium minutum*, *Islandinium? cezare*, *Islandinium brevispinosum* (Pospelova and Head, 2002), the cysts of *Polykrikos schwartzii* and *Polykrikos kofoidii* (Matsuoka et al., 2009), the cyst of *Protoperidinium fukuyoi* (Mertens et al., 2013), the cyst of *Scrippsiella trifida* (Head et al., 2006), and *Stelladinium bifurcatum* (Head et al., this issue).

Melitasphaeridium choanophorum is a new species in the database. It was accepted as ranging into the Holocene (Head and Westphal, 1999), but was subsequently confirmed as occurring in late Quaternary and surface sediment samples of the Gulf of Mexico (Limoges et al., 2013, 2014; Price et al., 2017), in late Quaternary (Mertens et al., 2009) and sediment trap samples (Bringué et al., 2018, 2019) of the Cariaco Basin, and Holocene sediments of the South China Sea (Li et al., 2017).

The cosmopolitan species *Operculodinium centrocarpum* sensu Wall and Dale (1966) shows considerable morphological variability especially in the length and number of processes. It refers to all modern morphotypes because the distinctions between them are arbitrary. This common Quaternary species should not be confused with *Operculodinium*

561
562
563 *centrocarpum* sensu stricto described from the Miocene of Australia and which has a
564
565 more robust morphology (see Paez-Reyes and Head, 2013 for discussion).
566
567

568
569 Several taxa are problematic because their diagnostic features are not obvious in optical
570
571 microscopy, especially in the case of poorly preserved material or folded specimens.
572
573 Among the problematic taxa, the round spiny brown cysts are difficult to distinguish in
574
575 routine analyses. They include species belonging mostly to the genera *Islandinium* and
576
577 *Echinidinium*, but a vast number of rare spiny brown cyst types belonging to a variety of
578
579 other genera also exist (see Mertens et al., this issue). The diagnostic features of the main
580
581 taxa from this group were described and illustrated by Radi et al. (2013) to help with
582
583 identification. However, some intraspecific gradational features often make it difficult to
584
585 be confident with identification. More critical is the fact that some species might have
586
587 been overlooked or grouped together during analyses of samples from the previous
588
589 databases.
590
591

592
593 Other taxa might have been identified with debatable taxonomic assignment. This is the
594
595 case for some *Spiniferites* taxa in the current database (de Vernal et al., 2018). Among
596
597 those, the taxonomic identities of *Spiniferites pachydermus* and *Spiniferites* sp. granular
598
599 type need to be clarified. *Spiniferites ramosus* remains with a lax definition, whereas
600
601 other species (*Spiniferites bulloideus*, *Spiniferites belerius*) have unclear distinctive
602
603 morphological characters and are often grouped with *Spiniferites ramosus* or *Spiniferites*
604
605 *membranaceus* (de Vernal et al., 2018; Mertens et al., 2018).
606
607

608
609 In the present paper, we provide and use data counts for all 71 taxa (Table S2). However,
610
611 for statistical treatments and the application of analogue techniques or transfer functions,
612
613
614
615
616

we recommend grouping taxa that could be misidentified during routine counts or that were not routinely discriminated in earlier versions of the database. Furthermore, we recommend not using some taxa with unclear taxonomical affinities such as Proteridinioids that group all unidentified brownish cysts (see Table 2 and above).

2.3 The environmental parameters

Sea surface temperature (SST), sea surface salinity (SSS), dissolved oxygen, and nutrients are from the World Ocean Atlas 2013 (WOA13; <https://www.nodc.noaa.gov/OC5/woa13/woa13data.html>). WOA13 is a dataset of objectively-analyzed fields of oceanographic conditions based on in-situ measurements with global coverage (Locarinini et al., 1013; Zweng et al., 2013). It provides a statistical mean and standard deviation at monthly averaging periods from January 1955 to December 2012 at one- to ¼-degree spatial resolution for temperature and salinity and at one-degree resolution for dissolved oxygen, nitrate, phosphate, and silicate. The WOA13 includes more data and less uncertainty than previous datasets of the World Ocean Atlas series (e.g., World Ocean Atlas 1994 to 2009 and the climatological atlas of Levitus, 1982), which were used in previous versions of the dinocyst database. The time interval from 1955 to 2012 included in the WOA13 version incorporates the most complete data coverage, with new regional and high-resolution data, especially in the Arctic, the northern North Pacific, the Greenland Sea, Iceland and Norwegian seas, and the northwest North Atlantic with a ¼-degree spatial resolution (https://www.nodc.noaa.gov/OC5/regional_climate/).

Sea-ice data are from the National Snow and Ice Data Center (NSIDC; Walsh et al., 2015). We used monthly averages from 1955 to 2012. Although the sea-ice data based on historical observations before the start of satellite measurements in 1979 are heterogeneous (Walsh and Chapman, 2001), the 1955 to 1979 interval includes an almost continuous Arctic-wide data record (Walsh et al., 2015). After 1979, all values are from satellite passive microwave sensors, providing a quasi-complete spatial and temporal coverage (Fetterer et al., 2017). Monthly sea-ice concentrations and extent compiled at a 1/4-degree resolution are available from the NSIDC website (<http://nsidc.org/data/G10010>). Here, the mean annual sea-ice concentration is expressed in percent of coverage, with values ranging from 0 to 100%, and seasonal sea-ice extent is expressed as the number of months with sea-ice concentration >50%.

The distance to the coast is expressed in km. It was calculated with ARCGIS using geodetic distances between features. The method is based on the World Geodetic System (WGS 84; <https://gisgeography.com/wgs84-world-geodetic-system/>), which takes into account the curvature of the spheroid and correctly deals with data near the date line and poles.

Bathymetry data are from the International Bathymetric Chart of the Arctic Ocean (Jakobsson et al., 2012) and the General Bathymetric Chart of the Oceans (GEBCO 2014, version 20141103, <http://www.gebco.net>).

Primary productivity data are calculated using the vertical generalized production model (VGPM) algorithm applied to the 2002–2017 chlorophyll data provided by NASA's Moderate Resolution Imaging Spectroradiometer (MODIS) program (<https://modis.gsfc.nasa.gov/data/dataproduct>). The VGPM is a “chlorophyll-based” model

that estimates ocean primary productivity from chlorophyll, SST, and photosynthetically active radiation (Behrenfield and Falkowski, 1997). The MODIS data have a 1/12-degree spatial resolution and monthly averages. As satellite observations may have coverage gaps due to polar night or clouds, data are missing in some regions. Areas with missing data were filled using simple linear interpolation within an 80 km radius. In Arctic regions, where winter data are missing and Arctic night prevails, we assumed zero primary productivity. For the n=1968 dataset, productivity values were extracted as average daily values for the four seasons (mgC/m²/day) and as annual total productivity (gC/m²/year) using ArcGIS software. Annual and monthly productivity data were downloaded from the Oregon State University website (<http://orca.science.oregonstate.edu/2160.by.4320.monthly.xyz.vgpm.m.chl.m.sst.php>).

Some of the 17 oceanographic parameters compiled here are correlated (see Table 3; Figure S1). This is the case for the two sea-ice parameters, which derive from the same measurements. This is also the case for winter and summer temperatures, sea ice and dissolved oxygen, the latter being strongly regulated by water temperature. Some productivity parameters also strongly correlate as do winter salinity with summer salinity, and distance to coast with bathymetry. However, the correlation between temperature and salinity is weak ($r < 0.41$; see Figure S1; Table 3). Hence, the n=1968 database offers a wide combination of environmental conditions and allows the simultaneous exploration of temperature and salinity gradients from nearshore to offshore settings and from sea-ice environments to tropical climates.

2.4 Multivariate analyses

Canonical ordination analyses were performed using CANOCO 5 software (ter Braak and Smilauer, 2012) to assess the effect of oceanographic variables on taxa occurrences. Variables assessed included bathymetry, distance to coast, SST, SSS, primary productivity (PP), dissolved oxygen, sea-ice cover and nutrient (phosphate, nitrate, silicate) concentrations. The analyses have been applied to the entire data set (71 taxa, 1968 sites and 17 sea surface parameters) and to two subsets of data obtained by separating the phototrophic taxa (41 taxa, 1926 sites) and heterotrophic taxa (30 taxa, 1895 sites). This separation was done to explore the respective difference in trophic behaviors, which may result in different ecological constraints. Another reason to separate the two types of taxa was to explore potential biases related to preservation as the cysts of many heterotrophic taxa are sensitive to degradation and selective preservation (e.g., Zonneveld et al., 2001, 2008).

The data were first analyzed using detrended correspondence analysis (DCA) by segments (Hill and Gauch, 1980) in order to estimate the gradient length of taxa turnover and thus to see if the data sets are structured on a linear or non-linear distribution. The first gradient (first DCA axis), given in standard deviation units, is close to or greater than four for the three data sets (see Table S4), which indicates a strong unimodal response and makes canonical correspondence analysis (CCA) an appropriate technique. CCA is a combination of regular multivariate analyses (correspondence analyses) and regressions. Results are presented in ordination and taxa diversity diagrams that express the pattern of variation in taxa compositions and the main relationships between taxa and oceanographic parameters.

The CCA results are interpreted using intra-dataset correlation matrices in which the relative importance of each parameter is given by the sign and magnitude of its correlation with ordination axes (Tables S3, S4). The interpretation is based on the variance explained by the canonical axes and the pseudo-canonical correlation, which respectively provide the strength and coherency of the relationship between scores of taxa and scores of hydrographic variables. Finally, the explained fitted variation represents the proportion of variance in taxon abundances that is related to oceanographic variables (Table 4).

To identify collinear parameters and avoid overinterpretation (Figure S1a–c), we performed CCA analyses using a 499-permutation test among the 17 environmental variables. The level of collinearity can be estimated from the variance inflation factor (VIF), which quantifies how much the statistical weight of a given variable is inflated due to collinearity or multicollinearity (e.g., Hair et al., 1995). VIF was computed for each environmental variable using the CANOCO software (ter Braak and Smilauer, 2012), as part of CCA analyses (Table 5). There is no consensus about the threshold under which collinearity can be safely ignored, but VIF values < 10 generally suggest that collinearity is not an issue (e.g., Neter et al., 1989). However, if a given environmental variable is completely colinear with other parameters, its VIF is set to 0 (ter Braak and Smilauer, 2012). For large datasets composed of many environmental parameters such as the n=1968 database, VIFs < 20 are acceptable (Jongman et al., 1995; ter Braak and Smilauer, 2012). The CCA permutation test indicates that three environmental variables record VIFs > 20 (Table 5). They include dissolved oxygen (VIF = 31.69) and the sea-ice parameters (VIF = 43.54 and 40.89). Annual productivity, which is the sum of seasonal

production, is also collinear with other productivity variables (VIF = 0; see Figure S1b). As further explored by Hohmann et al. (this issue), collinearity is problematic when using transfer functions based on regression models. However, it is not necessarily as problematic with the modern analogue techniques if the colinear parameters have known and distinct mechanisms for controlling species abundances. In any case, strong caution is needed when dealing with co-linear parameters (Juggins, 2013).

3. Results

3.1 The dinocyst assemblages

3.1.1 Overview

The dinocyst concentration in surface sediment samples varies by several orders of magnitudes from one site to another (Figure 2; Table S1). Many samples from the central Arctic Ocean and from offshore sites of the North Pacific and North Atlantic are characterized by extremely low cyst concentrations (< 10 cysts/g of dry sediment) and were excluded from the database as it was impossible to reach the minimal sum of 60 specimens (see above). Dinocysts are typically more abundant along continental margins than in offshore settings (Figure 2), but there is no clear relationship between bathymetry and dinocyst concentrations ($r < 0.15$). There is also no correlation between cyst concentration and productivity ($r < 0.1$). Although phototrophic dinoflagellates represent an important part of the phytoplanktonic productivity of the ocean (e.g., Simon et al., 2009), a direct relationship between dinocyst concentrations and net primary productivity is not predictable. Not only is the trophic behavior of dinoflagellates complex, including

phototrophy, heterotrophy and mixotrophy (e.g., Jeong et al., 2011), but not much more than about 12% produce distinctive cysts that fossilize in the sediment (e.g., Head, 1996). Hence, organic-walled dinoflagellate cysts provide a fragmentary picture of original populations, and phototrophic dinoflagellates represent only part of the primary production in the ocean. Nevertheless, although no quantitative relationship between dinocyst concentration and productivity can be established, high dinocyst abundances and fluxes necessarily require high biogenic production.

Dinocyst assemblages typically show a gradient of species richness from high to low latitudes (Figure 3). The proportions of phototrophic and heterotrophic taxa vary in space (Table 2, Figure 4) but there is no clear relationship with hydrographic (SSS, SST) or physiographic (distance to coast, bathymetry) parameters. Nevertheless, the highest proportions of heterotrophic taxa characterize the coastal zones of the eastern North Pacific marked by upwelling and the circum-Arctic where sea-ice cover develops seasonally (see also Radi and de Vernal, 2008).

3.1.2 Phototrophic taxa

Among phototrophic taxa, the most common are *Operculodinium centrocarpum*, *Nematosphaeropsis labyrinthus*, *Spiniferites elongatus*, *Spiniferites ramosus* and cysts of *Pentapharsodinium dalei*. Whereas *Operculodinium centrocarpum* is unquestionably cosmopolitan, *Nematosphaeropsis labyrinthus* and *Spiniferites ramosus* appear rarely in the Arctic Ocean (Figures 5a, 5c, 5e), and the cyst of *Pentapharsodinium dalei* and *Spiniferites elongatus* have a boreal–polar distributions (Figures 5d, 5e).

Among other common phototrophic taxa, *Impagidinium pallidum* is boreal–subarctic (Figure 5j), *Bitectadodinium tepikiense* and *Impagidinium sphaericum* occur mostly at mid-latitudes of the North Atlantic (Figures 5n, 5j) and *Pyxidinopsis reticulata* at mid-latitudes of the North Pacific (Figure 5p).

Other common taxa are distributed mostly in low to middle latitudes. They include *Spiniferites mirabilis*, *Spiniferites bentorii*, *Spiniferites membranaceus*, *Impagidinium aculeatum*, *Impagidinium patulum*, *Impagidinium strialatum*, *Impagidinium paradoxum* and *Lingulodinium machaerophorum* (Figures 5e, 5f, 5g, 5m). Some species such as *Spiniferites delicatus*, *Bitectatodinium spongium*, *Operculodinium israelianum*, *Polysphaeridium zoharyi*, *Tectadodinium pellitum* and *Tuberculodinium vancampoe* are mostly restricted to low latitude settings (Figures 5b, 5f, 5h, 5n–o). Many taxa occur in low abundances. Among those, some are cosmopolitan such as *Ataxiodinium choane* (Figure 5g), but others appear to be more characteristic of low- to mid-latitudes, notably *Impagidinium velorum* (Figure 5h), *Dalella chathamensis*, and *Melitasphaeridium choanophorum*.

3.1.3 Heterotrophic taxa

Among heterotrophic taxa, the genus *Brigantedinium* (Figure 5q) is by far the most cosmopolitan, occurring at all latitudes and from nearshore to offshore settings. While it is not very diagnostic as it is an opportunistic genus, its recovery from bottom sediments tends to indicate good preservation since it is sensitive to degradation by oxidation (Zonneveld et al., 2008). The circum-Arctic regions are characterized by abundant *Islandinium minutum* and the occurrence of *Islandinium? cezare* and *Echinidinium*

1065
1066
1067 *karaense* (Figures 5r, 5u). In low latitudes to subpolar environments of nearshore to
1068
1069 offshore settings, *Selenopemphix quanta* and *Trinovantedinium applanatum* (Figures 5s,
1070
1071 5v) are common. Most other peridinioid cysts, such as *Quinquecuspis concreta*, the cysts
1072
1073 of *Protoperidinium americanum* and *Protoperidinium fukuyoi*, *Echinidinium aculeatum*,
1074
1075 *E. granulatum* and *E. transparentum*, occur in coastal areas of low to middle latitudes
1076
1077 (Figures 5t, 5u, w, x). Many other peridinioid cysts occur in the sediments, but in low
1078
1079 abundance. They include *Selenopemphix nephroides*, *Xandarodinium xanthum*, the cyst of
1080
1081 *Protoperidinium stellatum*, *Votadinium spinosum* and *Votadinium calvum*.
1082
1083
1084

1085
1086 The order Gymnodiniales includes the cyst of *Gymnodinium catenatum* and closely
1087
1088 related forms, which were rarely recovered in the sediments and occur occasionally at
1089
1090 low to middle latitudes. The fossil record of the gymnodiniales is mostly represented by
1091
1092 the cyst of *Polykrikos kofoidii*, which is common in the Atlantic, and the cyst of
1093
1094 *Polykrikos schwartzii*, which is common in the Pacific. A morphologically similar cyst,
1095
1096 the Arctic morphotype of *Polykrikos?* sp., is characterized by squared outline of the
1097
1098 central body and a poorly ornamented cyst wall (Figure 5y). Because of its overall
1099
1100 appearance reminding that of cysts of *Polykrikos kofoidii* and because of common
1101
1102 occurrence in arctic environments (Figure 5y), it has been informally referred to as
1103
1104 *Polykrikos?* sp. – Arctic morphotypes (cf. Van Nieuwenhove et al., this issue). However,
1105
1106 phylogenetic analysis reveals that these cysts are associated with the Protoperidiniaceae
1107
1108 rather than the Gymnodiniales (Potvin et al., 2018).
1109
1110
1111

1112 3.2 Relationship between dinocyst assemblages and environmental parameters

1113
1114
1115
1116
1117
1118
1119
1120

The first three CCA axes explain 24.8, 21.1 and 20.6% of the total variance when using phototrophic, heterotrophic and all taxa, respectively (see Table 4a–c). Canonical correlations between CCA axes and dinocyst assemblages, with coefficients ranging from 0.7 to 0.96, reflect strong coherence between taxa distribution and oceanographic data while the explained fitted variance (74.6, 77.8 and 70.6%; Table 4a–c) indicates that the first three axes explain the large majority of the covariance between assemblages and environmental parameters. Regardless of the subset of data analyzed, dissolved oxygen content, which directly depends upon temperature, is the most determining parameter. The SSTs are the other parameters that explain most of the first CCA axis.

When using the entire data set with both phototrophic and heterotrophic taxa (71 taxa, 1968 sites), the first CCA axis explains 39.7% of the covariance and illustrates a positive correlation with sea ice and dissolved oxygen, and a negative correlation with SST (Table 4a, Figure 6). Hence, the ordination shows opposite trends between a group of taxa with affinities for polar and subpolar environment characterized by low temperatures such as the *Polykrikos?* sp – Arctic morphotypes, *Echinidinium karaense*, *Islandinium minutum*, *Spiniferites elongatus* and *Impagidinium pallidum* on one side, and another group of taxa with warmer water affinities including *Lingulodinium machaerophorum*, *Spiniferites delicatus* and *Spiniferites mirabilis*, on the other side. The second axis that explains 20.28% of the covariance is positively correlated to offshore conditions (high SSS, bathymetry and distance to shoreline) and negatively correlated to PP. Taxa with high positive CCA2 scores all belong to phototrophic taxa, notably *Impagidinium* species which also characterize oligotrophic environments. Almost all heterotrophic taxa have a negative CCA2 score and are related to high PP. The third axis explains 10.58% of the

covariance and shows weak correlations, positive with sea ice parameters and negative with productivity. The geographical distribution of the CCA axes 1, 2 and 3 clearly illustrates both latitudinal and nearshore to offshore gradients (Figure 7).

For the phototrophic taxa, the first axis (47.49% of the explained fitted variance) shows a very strong positive correlation ($r > 0.9$) with SSTs (Table 4b, Figure 6), with positive scores characterizing high species diversity. The negative scores mark low species diversity and the dominant occurrence of cysts of *Pentaparsodinium dalei*, *Impagidinium pallidum*, and *Spiniferites elongatus*, which thus correspond to cold conditions in polar and subpolar settings. The second axis explains 17.89% of the covariance. It is characterized by positive correlations with salinity and bathymetry, and by negative correlation with primary productivity, pointing to a nearshore (low SSS, high PP) to offshore (high SSS, low PP) gradient. Many *Impagidinium* taxa record positive scores whereas *Bitectatodinium spongium* and *Polysphaeridium zoharyi* have negative scores. The maximum species diversity is recorded in the warm and saline region of the ordination diagram. While one can distinguish “cold” and “warm” assemblages from negative and positive scores of the CCA1 respectively, the “warm” taxa group allows two subgroups to be highlighted from the CCA2 scores. One corresponds to positive CCA1 and CCA2. It is composed mainly of *Impagidinium velorum*, *Impagidinium paradoxum*, *Dalella chathamensis*, and *Impagidinium plicatum* and characterizes the oceanic and oligotrophic realm also marked by high SSS. The other “warm group” corresponds to positive CCA1 and negative CCA2. It comprises *Bitectatodinium spongium*, *Polysphaeridium zoharyi*, *Spiniferites pachydermus*, *Melitasphaeridium choanophorum* and *Nematosphaeropsis rigida*. It characterizes neritic sites with relatively low SSS and

high PP. The third axis explains only 8.79% of the covariance and show very weak correlations with the environmental parameters, the most significant being distance to coast and bathymetry.

The CCA results from the heterotrophic subset show that the first axis explains 50.8% of the covariance and corresponds to a positive correlation ($r > 0.85$) with SST and inverse relation with sea ice ($r \sim 0.74$). Whereas most taxa record positive scores, *Echinidinium karaense*, *Islandinium minutum*, *Islandinium? cezare* and *Polykrikos? sp.* – Arctic morphotypes are characterized by negative scores, thus illustrating affinities for cold waters and sea ice (Table 4b, Fig. 6). The second axis explains 15.61% of the covariance. It is characterized by slightly positive correlations with sea ice. The third axis that explains 12.8% of the covariance is best explained by showing a positive correlation to salinity and a negative correlation to productivity.

4. Discussion

4.1 Taphonomy and representativeness of dinocyst assemblages

The use of microfossils for paleoceanographic reconstructions relies on the assumption that assemblages in the sediments derive from production in the overlying water column and thus corresponds to vertical pelagic fluxes. The sinking of biogenic silt size particles occurs through processes involving phytodetritus aggregates, marine “snow” and fecal pellets (e.g., Beaulieu, 2002; Turner, 2002). Although the biological, physical and chemical mechanisms driving biogenic fluxes to the sea floor are complex and

discontinuous in space and time, the vertical fluxes generally increase with productivity (see review by Turner, 2015). Among the mechanisms involved, fecal pellets are a very efficient means for rapid settling, with fall rates reaching up to a thousand meters per day (Turner, 2015). Some heterotrophic dinoflagellates contribute to fecal pellet fluxes as they are directly associated with pellets on which they feed (e.g., Poulsen et al., 2011; Svensen et al., 2012). Moreover, both phototrophic and heterotrophic dinoflagellates and their cysts are ingested by grazers and incorporated with the pellets in which they sink, and possibly survive (e.g., Montresor et al., 2003). Phytodetritus aggregates, which are often associated with blooms, also foster rapid deposition (e.g., Beaulieu, 2002). Hence, whereas one cannot rule out the contemporaneous lateral transport of cysts in the water column and the nepheloid layer (Zonneveld et al., 2018), the sedimentation of dinocysts to the sea floor is usually intimately related to productivity in the overlying water column.

Preservation of organic-walled dinoflagellate cysts, which might affect taxa selectively through oxidation in the water column and at the water–sediment interface, is another source of uncertainty (e.g., Zonneveld et al., 2008). The cysts of heterotrophic taxa such as those of *Protoperidinium* and *Echinidinium* are particularly sensitive to oxidation (Zonneveld et al., 2001). In the n=1968 data set, heterotrophic taxa represent about 38% of the assemblages and occur in > 96% of the samples. The distribution of heterotrophic taxa relative to phototrophic taxa (Figures 4 and 6) seems to relate to ecological conditions and productivity, not necessarily to selective degradation. There is no clear correlation between the relative abundance of heterotrophic taxa and water depth ($r = 0.30$), where greater depths should theoretically foster oxidation through the water

column. Nevertheless, the ordination diagram from the CCA analysis with 71 taxa shows a cluster of heterotrophic species together with most primary productivity parameters in contrast to salinity, bathymetry and distance to the coast (Figure 6). This is particularly well expressed by the second axis of the CCA (see Figures 6–8). Furthermore, the results of CCA suggest that productivity, sea ice cover, and distance to coast appear to most strongly predict heterotrophic taxa distribution, not bathymetry (Figure 6c). Hence, it remains possible that selective degradation might impact the heterotrophic taxa, but the observed gradients from onshore to offshore settings are consistent with controls related to primary productivity and salinity (see also Figure 4).

4.2 Dinocyst assemblages as ecological and oceanographical tracers

One feature of the dinocyst database is that it encompasses estuarine, coastal, and offshore environments and represents large gradients of salinity, temperature and sea-ice cover. Hence the ecological domains documented by dinocyst assemblages are complex, making the transition from coastal areas to the open ocean. This is an advantage for environmental studies as different ecological variables can be assessed. However, this also creates challenges of interpretation due to the complex interactions between the multiple parameters.

Among the taxa of the n=1968 database, some show large plasticity for a wide range of environmental conditions as they are truly cosmopolitan and/or include several genetic entities with different ecological affinities. This is notably the case for *Brigantedinium* spp., which has a wide distribution but also includes several species. Among the commonly reported species, *Brigantedinium simplex* and *Brigantedinium cariacense*

appear cosmopolitan. This is also the case for *Operculodinium centrocarpum* sensu Wall and Dale (1966), which is among the most cosmopolitan of species (Van Nieuwenhove et al., this issue) but is known to include a wide range of gradational morphologies (e.g., de Vernal et al., 2001; Van Nieuwenhove et al., this issue) and probably encompasses several cryptic species (Mertens et al., 2012; Wang et al., 2019). In addition to *Brigantedinium* spp. and *Operculodinium centrocarpum* sensu Wall and Dale (1966), several taxa present a widespread distribution from temperate to Arctic or subarctic regions. They include the cyst of *Pentapharsodinium dalei*, *Ataxiodinium choane*, *Pyxidinosia reticulata*, *Spiniferites ramosus* and the cyst of *Polykrikos kofoidii*. In the case of the above-mentioned taxa, cryptic species may be involved with different ecological affinities. Nevertheless, many groups of taxa appear to be climatologically or ecologically significant. Hence, the CCA ordination diagrams (Figures 6–7) illustrate distribution patterns that allow at least four assemblage types to be clearly distinguished and reveal evident gradients with respect to temperature, salinity, sea-ice and productivity (see Figures 6–8).

1. In Arctic areas that experience sea ice, dinocyst assemblages in neritic settings are commonly characterized by *Islandinium minutum*, *Islandinium? cezare*, *Echinidinium karaense* and *Polykrikos? sp.* -Arctic morphotypes (positive axis 1, negative axis 2; Figures 6a, 7, 8).

2. In polar and subpolar environments of offshore settings marked by seasonal sea ice but high salinities, assemblages are commonly characterized by *Impagidinium pallidum* and *Spiniferites elongatus* (positive axes 1 and 2; Figures 6a, 7, 8).

3. In the tropical to temperate oceans, diversity is high. In the relatively high salinity zone that also corresponds to offshore and oligotrophic environments, phototrophic taxa dominate with the presence of several *Impagidinium* and *Spiniferites* species (negative axis 1, positive axis 2; Figures 6a, 7, 8). Such assemblages are mostly recorded in the Atlantic.

4. Finally, in nearshore settings of low latitudes marked by relatively low salinity and high primary productivity, assemblages are dominated by heterotrophic taxa, including most of the *Echinidinium* species and *Stelladinium* taxa, in addition to *Polysphaeridium zoharyi* and *Bitectatodinium spongium* (negative axes 1 and 2; Figures 6a, 7, 8). Such environments and assemblages predominantly characterize the Pacific regions.

The dinocyst assemblages are related to a combination of hydrographic parameters, among which SST, SSS, sea ice and productivity contribute significantly (Figures 6 and 8). However, the distribution of taxa and assemblages may also respond to other parameters that are not explored in this study, such as turbulence, stratification, current dynamics, nutrient stress, competition among species, etc. There are also regional specificities inherent to each sedimentary basin, which result in different interrelationships from one region to another, as exemplified in Radi and de Vernal (2008), Bonnet et al. (2010, 2011), Allan et al. (this issue) and Hohmann et al. (this issue). Hence, dinocyst assemblages are useful paleoceanographic and paleoecological indicators along the continental margins in general and seem to capture the regional differences between the Pacific and Atlantic, which are distinct with respect to their hydrographic properties.

4.3 Dinocyst assemblages and quantitative relationship with sea surface conditions

Dinocyst assemblages provide a picture of sea-surface conditions that is suitable for the application of transfer functions based on calibrations or analogue approaches, aiming at quantitative reconstruction of hydrographic parameters. However, beyond uncertainties related to taphonomic processes, there also may be temporal mismatches between the dinocyst assemblages and the hydrographic and productivity data. The surface sediment samples in which dinocyst assemblages were analyzed may represent fluxes over decades to several hundreds of years depending upon sedimentation rates and biological mixing. In contrast, the hydrographical and primary productivity data we used as reference represent the last decades, with a much higher density of values in recent times, when satellite observations provided high precision and continuous measurements. This temporal mismatch should not be a major problem if hydrographical variables are characterized by uniform conditions with oscillations around a steady average. However, ongoing global warming has already led to changes in sea surface temperature and sea ice cover (e.g., IPCC, 2013; Fisher et al., 2018), and anthropogenic activities have altered planktonic populations in the oceans (Jonkers et al. (2019) and likely modified ocean productivity (e.g., Moore et al., 2018). The temporal mismatch between assemblages from sediments and hydrographical information is therefore critical. Consequently, the transient state of the surface ocean may introduce biases in the apparent assemblage to hydrography relationships and in the use of any transfer functions or analogue method. This is a topic that deserves to be addressed in a further study.

5. Conclusions

In marine environments, dinoflagellates constitute an important part of eukaryotic phytoplankton together with the diatoms, haptophytes, and small prasinophytes (e.g., Not et al., 2012). Many dinoflagellates produce organic-walled cysts (dinocysts) that preserve in marine sediments and are recovered in palynological preparations. While dinocysts are less abundant in distal offshore settings, they occur in large numbers, up to 10^6 cysts g^{-1} , along the continental margins, where the assemblages capture gradients in salinity, temperature and/or sea-ice cover, in addition to primary productivity. The dinocyst database of the Northern Hemisphere, long used to study these relationships, now includes 1968 surface sediment samples and 71 taxa after standardization of laboratory procedure and taxonomic categories. The database contains 41 phototrophic taxa and 30 heterotrophic taxa. The maximum proportions of heterotrophic taxa being recorded in high-productivity regions such as sea-ice margin and upwelling environments. The assemblage distribution also shows both north–south and nearshore–offshore gradients, with maximum diversity of species along the continental margins and in warm temperate and tropical areas. Multivariate analyses furthermore demonstrate that sea-surface temperature and sea-ice are the most determining parameters in the distribution of dinocyst assemblages, regardless of their trophic behavior. A close relationship between phototrophic taxa distribution and onshore–offshore salinity gradients is an important feature of the database, as well as the strong linkages between the overall assemblage distribution and primary productivity in fall and winter.

Dinocysts are unique among micropaleontological proxies of sea-surface conditions because of their resistant wall composition and preservation in sediments. They are also unique because of the combination of marine environmental parameters that can be investigated simultaneously, as shown here. In particular, the possibility to disentangle salinity from temperature and productivity in surface waters is an asset for paleoceanographic studies. Over the past thirty years, much progress has been made regarding the distribution of dinocyst taxa relative to environmental conditions. A next stage is to extend the standardized database into the low latitudes and the Southern Hemisphere and further assess the impact of anthropogenic forcing on dinocyst-environment relationships.

References

- Aksu, A.E., 1983. Holocene and Pleistocene dissolution cycles in deep-sea cores of Baffin Bay and Davis Strait: Palaeoceanographic implications. *Marine Geology* 53, 331–348.
- Allan, E., de Vernal, A., Faurschou Knudsen, M., Hillaire-Marcel, C., Moros, M., Ribeiro, S., Ouellet-Bernier M.-M., Seidenkrantz, M.S., 2018. Late Holocene sea-surface instabilities in the Disko Bugt area, west Greenland, in phase with ^{18}O -oscillations at Camp Century. *Paleoceanography and Paleoclimatology* 33, 227–238.
- Allen, E., de Vernal, A., Krawczyk, D., Moros, M., Radi, T., Rochon, A., Seidenkrantz, M.S., Zaragosi, S., in rev. Distribution of dinocyst assemblages in surface sediment samples from the West Greenland margin. *Marine Micropaleontology* this issue.

Bé, A.W.H., Tolderlund, D.S., 1971. Distribution and ecology of living planktonic foraminifera in surface waters of the Atlantic and Indian oceans. In: Funnell, B.M., Riedel, W.R. (Eds.), *The Micropaleontology of Oceans*. Cambridge University Press, Cambridge, pp. 105–149.

Beaulieu, S.E., 2002. Accumulation and fate of phytodetritus on the sea floor. *Oceanography and Marine Biology: An Annual Review* 40, 171–232.

Behrenfeld, M.J., Falkowski, P.G., 1997. Photosynthetic rates derived from satellite-based chlorophyll concentration. *Limnology and Oceanography* 42, 1–20.

Beaulieu, S.E., 2002. Accumulation and fate of phytodetritus on the sea floor. *Oceanography and Marine Biology: An Annual Review* 40, 171–232.

Bonnet, S., de Vernal, A., Hillaire-Marcel, C., Radi, T., Husum, K., 2010. Variability of sea-surface temperature and sea-ice cover in the Fram Strait over the last two millennia. *Marine Micropaleontology* 74, 59–74.

Bonnet, S., de Vernal, A., Gersonde, R., Lembke-Jene, L., 2012. Modern distribution of dinocysts from the North Pacific Ocean (37–64°N, 144°E–148°W) in relation to hydrographic conditions, sea-ice and productivity. *Marine Micropaleontology* 84–85, 87–113.

Braarud, T., 1945. Morphological observations on marine dinoflagellate cultures (*Porella perforata*, *Goniaulax tamarensis*, *Protoceratium reticulatum*). *Avhandlingar utgitt av Det Norske Videnskaps-Akademi Oslo. I. Matematisk-Naturvidenskapelig Klasse* 1944 (11), 1–18.

Bringué, M., Thunell, B.C., Pospelova, V., Pinckney, J.L., Romero, O.E., Tappa, E.J., 2018. Physico-chemical and biological factors influencing dinoflagellate cyst production in the Cariaco Basin. *Biogeosciences* 15, 2325–2348.

- Bringué, M., Pospelova, V., Tappa, E.J., Thunell, R.C. 2019. Dinoflagellate cyst production in the Cariaco Basin: a 12 year-long sediment trap study. *Progress in Oceanography* 171, 175–211.
- Caron, M., Rochon, A., Montero-Serrano, J.-C., St-Onge, G. 2019. Evolution of sea-surface conditions on the northwestern Greenland margin during the Holocene. *Journal of Quaternary Science* 34(7), 569–580
- CLIMAP Project Members, 1976. The Surface of the Ice-Age Earth. *Science* 191, 1131–1137.
- Datema, M., Sangiorgi, F., de Vernal, A., Reichert, G.-J., Lourens LJ, Sluijs, A. 2017. Comparison of qualitative and quantitative dinoflagellate cyst approaches in reconstructing glacial–interglacial variability at the West Iberian Margin IODP 'Shackleton' Site U1385. *Marine Micropaleontology* 136, 14–29.
- de Vernal, A., Henry, M., Bilodeau, G., 2010. *Micropaleontological preparation techniques and analyses*. Les Cahiers du GEOTOP vol. 3, Third edition. Université du Québec à Montréal, Montréal. 31 pp.
- de Vernal, A., Marret, F., 2007. Organic-walled dinoflagellates : tracers of sea-surface conditions, In C. Hillaire-Marcel and A. de Vernal (eds.) *Proxies in Late Cenozoic Paleoceanography* Elsevier, pp. 371–408.
- de Vernal, A., Turon, J.-L., Guiot, J., 1994. Dinoflagellate cyst distribution in high latitude environments and quantitative reconstruction of sea-surface temperature, salinity and seasonality, *Canadian Journal of Earth Sciences* 31, 48–62.
- de Vernal, A., Hillaire-Marcel, C., Peltier, W.R., Weaver, A.J., 2002. The Structure of the Upper Water Column in the Northwest North Atlantic: Modern vs. Last Glacial Maximum Conditions. *Paleoceanography* 17, 1050.

de Vernal, A., Guiot, J., Turon, J.-L., 1993a. Postglacial evolution of environments in the Gulf of St. Lawrence: palynological evidence, *Géographie physique et Quaternaire* 47, 167–180.

de Vernal, A., Rochon, A., Hillaire-Marcel, C., Turon, J.-L., Guiot, J., 1993b. Quantitative reconstruction of sea-surface conditions, seasonal extent of sea-ice cover and meltwater discharges in high latitude marine environments from dinoflagellate cyst assemblages. In: *Proceedings of the NATO Workshop on Ice in the Climate System*, Springer-Verlag: Berlin, NATO ASI Series Vol. 112, 611–621.

de Vernal, A., Henry, M., Matthiessen, J., Mudie, P.J., Rochon, A., Boessenkool, K.P., Eynaud, F., Grøsfjeld, K., Guiot, J., Hamel, D., Harland, R., Head, M.J., Kunz-Pirrung, M., Levac, E., Loucheur, V., Peyron, O., Pospelova, V., Radi, T., Turon, J.-L., Voronina, E., 2001. Dinoflagellate cyst assemblages as tracers of sea-surface conditions in the northern North Atlantic, Arctic and sub-Arctic seas: the new “n = 677” database and its application for quantitative palaeoceanographic reconstruction. *Journal of Quaternary Science* 16, 681–698.

de Vernal, A., Eynaud, F., Henry, M., Hillaire-Marcel, C., Londeix, L., Mangin, S., Matthiessen, J., Marret, F., Radi, T., Rochon, A., Solignac, S., Turon, J.-L., 2005. Reconstruction of sea-surface conditions at middle to high latitudes of the Northern Hemisphere during the Last Glacial Maximum (LGM) based on dinoflagellate cyst assemblages. *Quaternary Science Reviews* 24, 897–924.

de Vernal, A., Rochon, A., Fréchette, B., Henry, M., Radi, T., Solignac, S., 2013a. Reconstructing past sea ice cover of the Northern Hemisphere from dinocyst assemblages: status of the approach. *Quaternary Science Reviews* 79, 122–134.

de Vernal, A., Hillaire-Marcel, C., Rochon, A., Fréchette, B., Henry, M., Solignac, S., Bonnet, S., 2013b. Dinocyst-based reconstructions of sea ice cover concentration during the Holocene in the Arctic Ocean, the northern North Atlantic Ocean and its adjacent seas. *Quaternary Science Reviews* 79: 111–121.

- de Vernal, A., Eynaud, F., Henry, M., Limoges A., Londeix, L., Matthiessen, J., Marret, F., Pospelova, V., Radi, T., Rochon, A., Van Nieuwenhove, N., Zaragosi, S., 2018. Distribution and (palaeo)ecological affinities of the main *Spiniferites* taxa in the mid–high latitudes of the Northern Hemisphere. *Palynology* 42, 182–202.
- Evitt, W. R., 1961. Observations on fossil dinoflagellates. *Micropaleontology* 7, 385–420.
- Evitt, W.R., Davidson, S.E., 1964. *Dinoflagellate studies I. Dinoflagellate cysts and Thecae*. Stanford University Publications, Geological Science 10, 1–12.
- Falardeau, J., de Vernal, A., Spielhagen, R., 2018. Paleoceanography of northeastern Fram Strait since the last glacial maximum: palynological evidence of large amplitude change. *Quaternary Science Reviews* 195, 133–152.
- Fetterer, F., Knowles, K., Meier, W. N., Savoie, M., Windnagel, A.K. 2017, updated daily. *Sea Ice Index, Version 3*. Boulder, Colorado USA. NSIDC: National Snow and Ice Data Center.
- Fisher, H., Meissner, K., Mix, A. et al., 2018. Palaeoclimate constraints on the impact of 2°C anthropogenic warming and beyond. *Nature Geoscience* 11, 474–485.
- Geitzenhauer, K.R., Roche, M., McIntyre, A., 1976. Modern Pacific coccolith assemblages: derivation and application to late Paleotemperature analyses. In Cline, R.M. & Hays, J.D. *Investigation of late Quaternary Paleoceanography and Paleoclimatology*. Geological Society of America Memoir 145, pp. 423–428.
- Grosfjeld, K., Harland, R., 2001. Distribution of modern dinoflagellate cysts from inshore areas along the coast of southern Norway. *Journal of Quaternary Science* 16, 651–659
- Guiot, J., de Vernal, A., 2007. Transfer functions: methods for quantitative paleoceanography based on microfossils. In: Hillaire-Marcel, C., de Vernal, A. (Eds.), *Proxies in Late Cenozoic Paleoceanography*. Elsevier, pp. 523–563.

- Guiot, J., de Vernal, A., 2011. Is spatial autocorrelation introducing biases in the apparent accuracy of paleoclimatic reconstructions? *Quaternary Science Reviews* 30, 1965–1972.
- Hair, J.F., Anderson, R.E., Tatham, R.L., Black, W.C., 1995. *Multivariate Data Analysis with Readings*, 4th ed., Prentice-Hall, Upper Saddle River, N.J., 745 pp.
- Hamel, D., de Vernal, A., Gosselin, M., Hillaire-Marcel, C., 2002. Organic-walled microfossils and geochemical tracers: sedimentary indicators of productivity changes in the North Water and northern Baffin Bay (High Arctic) during the last centuries. *Deep-Sea Research II* 49, 5277–5295.
- Harland, R., 1983. Distribution maps of Recent dinoflagellate cysts in bottom sediments from the North Atlantic Ocean and adjacent seas. *Palaeontology* 26, 321–387.
- Head, M. J., 1996. Modern dinoflagellate cysts and their biological affinities. In: J. Jansonius & D. C. McGregor (Eds), *Palynology: Principles and applications*. American Association of Stratigraphic Palynologists Foundation, Vol. 3, pp. 1197–1248.
- Head, M. J., Mantilla-Duran, F., in press. *Atlanticodinium striaticonulum* n. gen., n. sp., a widespread extant dinoflagellate cyst from the late Cenozoic, and its comparison with *Atlanticodinium janduchenei* (Head et al., 1989) n. comb. *Marine Micropaleontology* this issue.
- Head, M.J., Westphal, H. 1999. Palynology and paleoenvironments of a Pliocene carbonate platform: the Clino Core, Bahamas. *Journal of Paleontology* 73(1), 1–25.
- Head, M.J., Lewis, J., de Vernal, A., 2006. The cyst of the calcareous dinoflagellate *Scrippsiella trifida*, and the fossil record of its organic wall, *Journal of Palaeontology* 80, 1–18.
- Head, M.J., Harland, R., Matthiessen, J., 2001. Cold marine indicators of the late Quaternary: the new dinoflagellate cyst genus *Islandinium* and related morphotypes. *Journal of Quaternary Science* 16, 621–636.

- Head, M.J., Pospelova, V., Radi, T., and Marret, F., in press. *Stelladinium bifurcatum* n. sp., a distinctive extant heterotrophic dinoflagellate cyst from the late Quaternary of the eastern Pacific and east equatorial Atlantic oceans. *Marine Micropaleontology*, this issue.
- Heikkilä, M., Pospelova, V., Hochheim, K.P., Kuzyk, Z.Z.A., Stern, G.A., Barber, D.G., Macdonald, R.W., 2014. Surface sediment dinoflagellate cysts from the Hudson Bay system and their relation to freshwater and nutrient cycling. *Marine Micropaleontology* 106, 79–109.
- Hill, M. O., Gauch, H. G. 1980. Detrended correspondence analysis, an improved ordination technique. *Vegetario* 42, 47–58.
- Hillaire-Marcel, C., de Vernal, A., Bilodeau, G., Weaver, A.J., 2001. Absence of deep-water formation in the Labrador Sea during the last interglacial period. *Nature* 410, 1073–1077.
- Imbrie, J., Kipp, N. G., 1971. A new micropaleontological method for quantitative paleoclimatology: Application to a late Pleistocene Caribbean core. In: Turekian, K.K. (ed.), *The Late Cenozoic Glacial Ages* Yale University Press, New Haven, 71–181.
- IPCC, 2013. *Climate Change 2013: The Physical Science Basis* (Eds. Stocker, T. F. et al.), Cambridge Univ. Press.
- Jakobsson, M., Mayer, L.A., Coakley, B., Dowdeswell, J.A., Forbes, S., Fridman, B., Hodnesdal, H., Noormets, R., Pedersen, R., Rebesco, M., Schenke, H.W., Zarayskaya, Y., Accettella, D., Armstrong, A., . Anderson, R.M., Bienhoff, P., Camerlenghi, A., Church, I., Edwards, M., Gardner, J.V., Hall, J.K.; Hell, B., Hestvik, O., Kristoffersen, Y., Marcussen, C., Mohammad, R., Mosher, D., Nghiem, S.V., Pedrosa, M.T., Travaglini, P.G., Weatherall, P., 2012. The International Bathymetric Chart of the Arctic Ocean (IBCAO) Version 3.0. *Geophysical Research Letters* 39, L12609.

- Jeong, H. J., Yoo, Y. D., Kim, J. S., Seong, K. A., Kang, N. S., Kim, T. H., 2010. "Growth, feeding and ecological roles of the mixotrophic and heterotrophic dinoflagellates in marine planktonic food webs". *Ocean Science Journal* 45: 65–91.
- Jongman, R.H.G., ter Braak, C.J.F., Van Tongeren, O.F.R., 1995. *Data Analysis in Community and Landscape Ecology*. Cambridge University Press, Cambridge. 299 pp.
- Jonkers, L., Hillebrandt, H., Kucera, M., 2019. Global change drives modern plankton communities away from the pre-industrial state. *Nature* 570: 372–375.
- Juggins, S., 2013. Quantitative reconstructions in paleolimnology: new paradigm or sick science? *Quaternary Science Reviews* 64, 20–32.
- Hohmann, S., Kucera, M., de Vernal, A., in rev. Identifying the signature of surface-ocean properties in dinocyst assemblages: Implications for quantitative paleoceanographical reconstructions by transfer functions and analogue techniques. *Marine Micropaleontology* this issue.
- Kucera, M., Rosell-Melé, A., Schneider, R., Waelbroeck, C., Weinelt, M., 2005. Multiproxy approach for the reconstruction of the glacial ocean surface (MARGO). *Quaternary Science Reviews* 24, 813–819.
- Kunz-Pirrung, M., Matthiessen, J., de Vernal, A., 2001. Late Holocene dinoflagellate cysts as indicators of short-term climate variability in the eastern Laptev Sea (Arctic Ocean). *Journal of Quaternary Science* 16, 711–717.
- Levitus, S., 1982. *Climatological Atlas of the World Ocean*, NOAA/ERL GFDL professional paper 13, Princeton N.J. 173 pp.
- Li, Z., Pospelova, V., Lin, H.-L., Liu, L., Song, B., 2018. Seasonal dinoflagellate cyst production and terrestrial palynomorph deposition in the monsoon influenced South China Sea: A sediment trap study from the Southwest Taiwan waters. *Review of Palaeobotany and Palynology* 257, 117–139.

- Limoges, A., de Vernal, A., Van Nieuwenhove, N., 2014. Long-term hydrological changes in the northeastern Gulf of Mexico (ODP-625B) during the Holocene and late Pleistocene inferred from organic-walled dinoflagellate cysts. *Palaeogeography, Palaeoclimatology, Palaeoecology* 414, 178–191.
- Limoges, A., Kieft, J.-F., Radi, T., Ruíz-Fernandez, A.C., de Vernal, A., 2010. Dinoflagellate cyst distribution in surface sediments along the south-western Mexican coast (14.76° N to 24.75°N). *Marine Micropaleontology* 76, 104–123.
- Limoges, A., Londeix, L., de Vernal, A., 2013. Organic-walled dinoflagellate cyst distribution in the Gulf of Mexico. *Marine Micropaleontology* 102, 51–68.
- Limoges, A., Ribeiro, S., Weckström, K., Heikkilä, M., Zamelczyk, K., Andersen, T. J., Tallberg, P., Guillaume Massé, G., Rysgaard, S., Nørgaard-Pedersen, N., Seidenkrantz, M.-S., 2018. Linking the modern distribution of biogenic proxies in High Arctic Greenland shelf sediments to sea ice, primary production, and Arctic–Atlantic inflow. *Journal of Geophysical Research: Biogeosciences* 123, 760–786.
- Limoges, A., Van Nieuwenhove, N., Mertens, K.N., Head, M.J., Pospelova, V., Rochon, A. A review of rare or not well known extant marine organic-walled dinoflagellate cyst taxa of the orders Gonyaulacales and Suessiales from the Northern Hemisphere. *Marine Micropaleontology* this issue.
- Locarnini, R. A., Mishonov, A.V., Antonov, J.I., Boyer, T.P., Garcia, H.E., Baranova, O.K., Zweng, M.M., Paver, C.R., Reagan, J.R., Johnson, D.R., Hamilton, M., Seidov, D. 2013. World Ocean Atlas 2013, Volume 1: Temperature. S. Levitus, Ed., A. Mishonov Technical Ed.; *NOAA Atlas NESDIS* 73, 40 pp.
- Marret, F., Scourse, J., Kennedy, H., Ufkes, E., Jansen, J.F., 2008. Marine production in the Congo influenced SE Atlantic over the past 30,000 years: A novel dinoflagellate-cyst based transfer function approach. *Marine Micropaleontology* 68, 198–222.

Maynard, N.G., 1976. Relationship between diatoms in surface sediments of the Atlantic Ocean and the biological and physical oceanography of overlying waters. *Paleobiology* 2, 99–121.

Matsuoka, K., Kawami, H., Nagai, S., Iwataki, M., Takayama, H., 2009. Re-examination of cyst–motile relationships of *Polykriko skofoidii* Chatton and *Polykriko sschwartzii* Bütschli (Gymnodiniales, Dinophyceae). *Review of Palaeobotany and Palynology* 154, 79–90.

Mertens, K., Bringué, M., Van Nieuwenhove, N., Takano, Y., Pospelova, V., Rochon, A., de Vernal, A., Radi, T., Dale, B., Patterson, R.T., Weckström, K., Andrén, E., Louwye, S., Matsuoka, K., 2012. Process length variation of the cyst of the dinoflagellate *Protoceratium reticulatum* in the North Pacific and Baltic–Skagerrak region: calibration as an annual density proxy and first evidence of pseudo-cryptic speciation. *Journal of Quaternary Science* 27, 734–744.

Mertens, K.N., González, C., Delusina, I., Louwye, S., 2009b. 30 000 years of productivity and salinity variations in the late Quaternary Cariaco Basin revealed by dinoflagellate cysts. *Boreas* 38, 647–662.

Mertens, K.N., Yamaguchi, A., Takano, Y., Pospelova, V., Head, M.J., Radi, T., Pieńkowski, A.J., de Vernal, A., Kawami, H., Matsuoka, K., A., 2013. New Heterotrophic Dinoflagellate from the Northeastern Pacific, *Protoperidinium fukuyoi*: Cyst–Theca Relationship, Phylogeny, Distribution and Ecology. *Journal of Eukaryotic Microbiology* 60, 545–563.

Mertens, K.N., Van Nieuwenhove, N., Gurdebeke, P.R., Aydin, H., Bogus, K., Bringué, M., Dale, B., De Schepper, S., de Vernal, A., Ellegaard, M., Grothe, A., Gu, H., Head, M.J., Heikkilä, M., Limoges, A., Londeix, L., Louwye, S., Marret, F., Masure, E., Matsuoka, K., Mudie, P.J., Penaud, A., Pospelova, V., Price, A.M., Ribeiro, S., Rochon, A., Sangiorgi, F., Schreck, M., Torres, V., Uzar, S., Versteegh, G.J.M., Warny, S., Zonneveld, K., 2018. The dinoflagellate cyst genera *Achomosphaera* Evitt 1963 and

Spiniferites Mantell 1850 in Pliocene to modern sediments: a summary of round table discussions. *Palynology* 42, 10–44.

Mertens, K.N., Gu, H., Gurdebeke, P.R., Takano, Y., Clarke, D., Aydin, H., Li, Z., Pospelova, V., Matsuoka, K., Head, M.J., in press. A review of rare and endemic extant marine organic-walled dinoflagellate cyst taxa of the orders Gymnodiniales and Peridiniales from the Northern Hemisphere. *Marine Micropaleontology*, this issue.

Montresor, M., Nuzzo, L., Mazzochi, M.G., 2003. Viability of dinoflagellate cysts after the passage through the copepod gut. *Journal of Experimental Marine Biology and Ecology* 287, 209–221.

Moore, J.K., Fu, W., Primeau, F. et al, 2018. Sustained climate warming drives declining marine biological productivity. *Science* 359: 1139–1143.

Mudie P.J., Short S.K., 1985. Marine palynology of Baffin Bay. In: Andrews J.T. (ed.) *Quaternary Environments*, Allen & Unwin: Boston, London, Sydney, 263–308.

Neter, J., Wasserman, W., Kutner, M.H., 1989. *Applied Linear Regression Models*, 2nd ed., Irwin, Homewood, IL., 667 pp.

Nordli, E., 1951. Resting spores in *Goniaulax polyedra* Stein. *NyttMagasin for Naturvidenskapene* 88, 207–212.

Not, F., Siano, R., Kooistra, W.H.C.F., Simon, N., Vaulot, D., Probert, I., 2012. Diversity and ecology of eukaryotic marine phytoplankton. In: Jacquot, J.P., and Gadal, P. (eds). *Genomic insights into the biology of algae*. Amsterdam, pp. 1–53.

Paez-Reyes, M., Head, M.J., 2013. The Cenozoic gonyaulacacean dinoflagellate genera *Operculodinium* Wall, 1967 and *Protoceratium* Bergh, 1881 and their phylogenetic relationships. *Journal of Paleontology* 87, 786–803.

- Pospelova, V., Chmura, G.L., Boothman, W.S., Latimer, J.S., 2005. Spatial distribution of modern dinoflagellate cysts in polluted estuarine sediments from Buzzards Bay (Massachusetts, USA) embayments. *Marine Ecology Progress Series* 292, 23–40.
- Pospelova, V., de Vernal, A., Pedersen, T., 2008. Distribution of dinoflagellate cysts in surface sediments from the northeastern Pacific Ocean (43–25°N) in relation to sea-surface temperature, salinity, productivity and coastal upwelling. *Marine Micropaleontology* 68, 21–48.
- Pospelova, V., Head, M.J., 2002. *Islandinium brevispinosum* sp. nov. (Dinoflagellata), a new organic-walled dinoflagellate cyst from modern estuarine sediments of New England (USA). *Journal of Phycology* 38, 593–601.
- Potvin, É., Kim, S.-Y., Yang, E.J., Head, M.J., Kim, H.-C., Nam, S.-I., Yim, J.H., Kang, S.-H., 2018. *Islandinium minutum* subsp. *barbatum* subsp. nov. (Dinoflagellata), a new organic-walled dinoflagellate cyst from the western Arctic: morphology, phylogenetic position based on SSU rDNA and LSU rDNA, and distribution. *Journal of Eukaryotic Microbiology* 65, 750–772.
- Poulsen, L.K., Moldrup, M., Berge, T., Hansen, P.J., 2011. Feeding on copepod fecal pellets: a new trophic role of dinoflagellates as detritivores. *Marine Ecology Progress Series* 441, 65–78.
- Price, A.M., Pospelova, V., Coffin, M.R.S., Latimer, J.S. and Chmura, G.L., 2016. Biogeography of dinoflagellate cysts in northwest Atlantic estuaries. *Ecology and Evolution* 6, 5648–5662.
- Price, A.M., Baustian, M.M., Turner, R.E., Rabalais, N.N., Chmura, G.L., 2017a. *Melitasphaeridium choanophorum*— a living fossil dinoflagellate cyst in the Gulf of Mexico. *Palynology* 41, 351–358.
- Price, A.M., Coffin, M.R.S., Pospelova, V., Latimer, J.S., Chmura, G.L., 2017b. Effect of nutrient pollution on dinoflagellate cyst assemblages across estuaries of the NW Atlantic. *Marine Pollution Bulletin* 121, 339–351.

- Price, A.M., Baustian, M.M., Turner, R.E., Rabalais, N.N. and Chmura, G.L., 2018. Dinoflagellate cysts track eutrophication in the northern Gulf of Mexico. *Estuaries and Coasts*, 41, 1322–1336.
- Radi, T., de Vernal, A., 2004. Dinocyst distribution in surface sediments from the northeastern Pacific margin (40–60°N) in relation to hydrographic conditions, productivity and upwelling. *Review of Palaeobotany and Palynology* 128, 169–193.
- Radi, T., de Vernal, A., 2008. Dinocysts as proxy of primary productivity in mid–high latitudes of the Northern Hemisphere. *Marine Micropaleontology* 68, 84–114.
- Radi, T., Pospelova, V., de Vernal, A., Vaughn, B.J., 2007. Dinoflagellate cysts as indicators of water quality and productivity in estuarine environments of British Columbia. *Marine Micropaleontology* 62, 269–297.
- Radi, T., de Vernal, A., Peyron, O., 2001. Relationships between dinocyst assemblages in surface sediment and hydrographic conditions in the Bering and Chukchi seas. *Journal of Quaternary Science* 16, 667–681.
- Radi, T., Bonnet, S., Cormier, M.A., de Vernal, A., Durantou, L., Faubert, E., Head, M.J., Henry, M., Pospelova, V., Rochon, A., Van Nieuwenhove, N., 2013. Operational taxonomy and (paleo)-autecology of round, brown, spiny dinoflagellate cysts from the Quaternary of high northern latitudes. *Marine Micropaleontology* 74, 59–74.
- Richerol, T., Rochon, A., Blasco, S., Scott, D.B., Schell, T.M., Bennett, R.J., 2008a. Distribution of dinoflagellate cysts in surface sediments of the Mackenzie Shelf and Amundsen Gulf, Beaufort Sea (Canada). *Journal of Marine Systems* 74, 825–839.
- Rochon, A., de Vernal, A., Turon, J.-L., Matthiessen, J., Head, M.J., 1999. *Distribution of recent dinoflagellate cysts in surface sediments from the North Atlantic Ocean and adjacent seas in relation to sea-surface parameters*. AASP Foundation Contribution Series Vol. 35, 1–152.

- Rossignol, M., 1964. Hystrichosphères du Quaternaire en Méditerranée orientale, dans les sédiments pléistocènes et les boues marines actuelles. *Rev. Micropaleontol.* 7, 83–99.
- Sach, H.M., 1973. North Pacific radiolarian assemblages and their relationship to oceanographic parameters. *Quaternary Research* 3, 73–88.
- Sancetta, C.A., 1977. *Oceanography of the North Pacific during the last 18,000 years derived from fossil diatoms*. PhD thesis, Oregon State University, Corvallis 148 p.
- Simon, N., Cras, A.L., Foulon, E., Lemée, R., 2009. Diversity and evolution of marine phytoplankton *Comptes rendus biologie* 332, 159–170.
- Solignac, S., Grøsfjeld, K., Giraudeau, J., de Vernal, A., 2009. Distribution of recent dinocyst assemblages in the western Barents Sea *Norwegian Journal of Geology* 89, 109–119.
- Sundqvist, H.S., Kaufman, D.S., McKay, N.P., Balascio, N.L., Briner, J.P., Cwynar, L.C., Sejrup, H.-P., Seppä, H., Subetto, D.A., Andrews, J.T., Axford, Y., Bakke, J., Birks, H.J.B., Brooks, S.J., de Vernal, A., Jennings, A., Ljungqvist, F.C., Ruhland, K.M., Saenger, C., Smol, J.P., Viau, A. (2014) Arctic Holocene proxy climate database – New approaches to assessing geochronological accuracy and encoding climate variables *Climate of the Past* 10, 1–63.
- Svensen, C., Wexels Riser, C., Reigstad, M., Seuthe, L., 2012. Degradation of copepod faecal pellets in the upper layer: role of microbial community and *Calanus finmarchicus*. *Marine Ecology Progress Series* 462, 39–49.
- Ter Braak, C.J.F., Smilauer, P., 2012. *Canoco reference manual and user's guide: software for ordination* (version 5). Microcomputer Power (Ithaca, NY, USA), 496 pp.
- Traverse, A., 1988. *Paleopalynology*. Allen & Unwin, 600 p.

Turner, J.T., 2002. Zooplankton fecal pellets, marine snow and sinking phytoplankton blooms. *Aquatic Microbial Ecology* 27, 57–102.

Turner, J.T., 2015. Zooplankton fecal pellets, marine snow, phytodetritus and the ocean's biological pump. *Progress in Oceanography* 130, 205–248.

Turon J-L. 1984. *Le palynoplancton dans l'environnement actuel de l'Atlantique nord-oriental. Évolution climatique et hydrologique depuis le dernier maximum glaciaire.* Doctorat ès sciences thesis, Université Bordeaux I, Mémoire de l'Institut de Géologie du Bassin d'Aquitaine 17, 313 p.

Vásquez-Bedoya, L.F., Radi, T., Ruiz-Fernández, A.C., de Vernal, A., Machain-Castillo, M.L., Kieft, J.F., Hillaire-Marcel, C., 2008. Centennial record of organic-walled dinoflagellate cysts and benthic foraminifera in coastal sediments from the Gulf of Tehuantepec, eastern equatorial Pacific. *Marine Micropaleontology* 68, 49–65.

Van Nieuwenhove, N., Hillaire-Marcel, C., Bauch, H.A., de Vernal, A., 2016. Sea surface density gradients in the Nordic seas during the Holocene as revealed by paired microfossil and isotope proxies. *Paleoceanography* 31, 380–398.

Voronina, E., Polyak, L., de Vernal, A., Peyron., O., 2001. Holocene variations of sea-surface conditions in the southeastern Barents Sea based on palynological data. *Journal of Quaternary Science* 16, 717–727.

Waelbroeck, C., Paul, A., Kucera, M., Rosell-Melé, A., Weinelt, M., Schneider, R., Mix, A. C., Abelmann, A., Armand, L., Bard, E., Barker, S., Barrows, T. T., Benway, H., Cacho, I. , Chen, M.-T., Cortijo, E. , Crosta, X., de Vernal, A., Dokken, T., Duprat, J., Elderfield, H., Eynaud, F., Gersonde, R., Hayes, A., Henry, M., Hillaire-Marcel, C., Huang, C.-C., Jansen, E., Juggins, S., Kallel, N., Kiefer, T., Kienast, M., Labeyrie, L., Leclaire, H., Londeix, L., Mangin, S., Matthiessen, J., Marret, F., Meland, M., Morey, A. E., Mulitza, S., Pflaumann, U., Pisias, N. G., Radi, T., Rochon, A., Rohling, E. J., Saffi, L., Schäfer-Neth, C., Solignac, S., Spero, H., Tachikawa, K.,

- Turon, J.-L., 2009. Constraints on the magnitude and patterns of ocean cooling at the Last Glacial Maximum, *Nature Geoscience* 2, 127–132.
- Wall, D., 1965. Modern hystrichospheres and dinoflagellate cysts from the Woods Hole region. *Grana* 6, 297–314,
- Wall, D., Dale, B., 1968. Modern dinoflagellate cysts and evolution of the Peridinales. *Micropaleontology* 14, 265–304.
- Wall, D., Dale, B., Lohmann, G.P., Smith, W.K., 1977. The environmental and climatic distribution of dinoflagellate cysts in modern marine sediments from regions in the North and South Atlantic Oceans and adjacent seas. *Marine Micropaleontology* 2, 121–200.
- Walsh, J.E., Chapman, W.L., 2001. 20th-century sea-ice variations from observational data. *Annals of Glaciology* 33. <http://dx.doi.org/10.3189/172756401781818671>.
- Walsh, J.E., Chapman, W.L., Fetterer, F., 2015. updated 2016. *Gridded Monthly Sea Ice Extent and Concentration, 1850 Onward, Version 1*. Boulder, Colorado USA. NSIDC: National Snow and Ice Data Center. doi: <https://doi.org/10.7265/N5833PZ5>.
- Wang, N., Mertens, K.N., Krock, B., Luo, Z., Derrien, A., Pospelova, V., Liang, Y., Bilien, G., Smith, K.F., De Schepper, S., Wietkamp, S., Tillmann, U., Gu, H., 2019. Cryptic speciation in *Protoceratium reticulatum* (Dinophyceae): Evidence from morphological, molecular and ecophysiological data. *Harmful Algae* <https://doi.org/10.1016/j.hal.2019.05.003>.
- Williams, D.B., 1971. The occurrence of dinoflagellates in marine sediments. In: Funnell, B.M., Riedel, W.R. (Eds.), *The Micropalaeontology of Oceans*. Cambridge University Press, Cambridge, pp. 231–243. □
- Williams, G.L., Fensome, R.A. and MacRae, R.A., 2017. *The Lentin and Williams index of fossil dinoflagellates 2017 edition*. American Association of Stratigraphic Palynologists Contributions Series, no. 48.

Zonneveld, K.A.F., Marret, F., Versteegh, G.J.M., Bonnet, S., Bouimetarhan, I., Crouch, E., de Vernal, A., Elshanawany, R., Edwards, L., Esper, O., Forke, S., Grøsfjeld, K., Henry, M., Holzwarth, U., Kielt, J.-F., Kim, S.-Y., Ladouceur, S., Ledu, D., Chen, L., Limoges, A., Londeix, L., Lu, S.-H., Mahmoud, M.S., Marino, G., Matsouka [sic], K., Matthiessen, J., Mildenhall [sic], D.C., Mudie, P., Neil, H.L., Pospelova, V., Qi, Y., Radi, T., Richerol, T., Rochon, A., Sangiorgi, F., Solignac, S., Turon, J.-L., Verleye, T., Wang, Y., Wang, Z., Young, M., 2013. Atlas of modern dinoflagellate cyst distribution based on 2405 datapoints. *Review of Palaeobotany and Palynology* 191, 1–197.

Zonneveld, K.A.F., Ebersbach, F., Maekea, M., Versteegh, G.J.M., 2018. Transport of organic-walled dinoflagellate cysts in nepheloid layers off Cape Blanc (N-W Africa). *Deep-Sea Research I* 139, 55–67.

Zonneveld, K.A.F., Versteegh, G.J.M., Kodrans-Nsiah, M., 2008. Preservation and organic chemistry of Late Cenozoic organic-walled dinoflagellate cysts: A review. *Marine Micropaleontology* 86, 179–197.

Zonneveld, K.A.F., Versteegh, G.J.M., de Lange, G.J., 2001. Palaeoproductivity and post-depositional aerobic organic matter decay reflected by dinoflagellate cyst assemblages of the Eastern Mediterranean S1 sapropel. *Marine Geology* 172, 181–195.

Zweng, M.M., Reagan, J.R., Antonov, J.I., Locarnini, R.A., Mishonov, A.V., Boyer, T.P., Garcia, H.E., Baranova, O.K., Johnson, D.R., Seidov, D., Biddle, M.M., 2013. World Ocean Atlas 2013, Volume 2: Salinity. S. Levitus, Ed., A. Mishonov Technical Ed.; *NOAA Atlas NESDIS 74*, 39 pp.

Acknowledgements

This study is the result of a long-term endeavor led by AdV, which was supported by the Natural Sciences and Engineering Research Council (NSERC) of Canada and the *Fonds*

2577
2578
2579 *de recherche du Québec – Nature et Technologie (FRQNT)*. SDS is funded by
2580
2581 Research Council of Norway project 268062 (aDNAPROX). Samples in the Greenland
2582
2583 Sea were collected by participants of the Ice2Ice project, funded from the
2584
2585 European Research Council under the European Community's Seventh Framework
2586
2587 Program (FP7/2007-2013) / ERC grant agreement 610055. This work was also supported
2588
2589 in part by the Zuckerman STEM Leadership Program through a postdoctoral fellowship
2590
2591 to AP. We are extremely grateful to all colleagues who helped us to access surface
2592
2593 sediment samples and to all students and research personnel who contributed to sample
2594
2595 preparation and/or analyses at the microscope. We also thank the anonymous reviewers
2596
2597 and the editor of the Journal for their helpful comments and suggestions.
2598
2599
2600
2601
2602
2603
2604
2605
2606
2607
2608
2609
2610
2611
2612
2613
2614
2615
2616
2617
2618
2619
2620
2621
2622
2623
2624
2625
2626
2627
2628
2629
2630
2631
2632

FIGURE CAPTIONS

Figure 1. Geographical incremental distribution of surface sediment samples and the main updates of the Northern Hemisphere standardized dinocyst database: n = 371 (Rochon et al., 1999), n=677 (de Vernal et al., 2001), n=940 (de Vernal et al., 2005), n=1171 (Radi and de Vernal, 2008), n=1492 (de Vernal et al., 2013a), n=1968 (this study).

Figure 2. Dinocyst concentrations in surface sediment samples. Concentrations were reported as number of specimens per unit of volume (cm³) or dry weight (gram) of sediment (see Table S1 for the values and their corresponding units).

Figure 3. The number of identified dinocyst taxa in the samples of the n=1968 database.

Figure 4. The proportion of phototrophic vs heterotrophic taxa in the dinocyst assemblages expressed as the percentages of phototrophs.

Figure 5. The percentages of the main dinocyst taxa (for data, see Table S2)

(a) *Operculodinium centrocarpum* sensu Wall and Dale (1966); (b) *Operculodinium israelianum*, *Atlanticodinium striaticonulum*, *Operculodinium longispinigerum*, *Operculodinium giganteum*; (c) *Nematosphaeropsis labyrinthus* and *Nematosphaeropsis rigida*; (d) cyst of *Pentapharsodinium dalei*; (e) *Spiniferites elongatus*, *Spiniferites ramosus*, *Spiniferites mirabilis-hyperacanthus*; (f) *Spiniferites membranaceus*, *Spiniferites bentorii*, *Spiniferites delicatus*, *Spiniferites belerius*, *Spiniferites bulloideus*; (g) *Ataxiodinium choane*; (h) *Tuberculodinium vancampoe*; (i) *Impagidinium aculeatum*, *Impagidinium paradoxum*, *Impagidinium patulum*, *Impagidinium striatum*; (j) *Impagidinium pallidum*, *Impagidinium sphaericum*; (k) *Impagidinium plicatum*, *Impagidinium velorum*; (l) cyst of *Scrippsiella trifida*; (m) *Lingulodinium machaerophorum*; (n) *Bitectatodinium tepikiense* and *Bitectatodinium spongium*; (o) *Polysphaeridium zoharyi*; (p) *Pyxidinosia reticulata*; (q) *Brigantedinium* spp.; (r) *Islandinium minutum*, *Islandinium? cezare* and *Islandinium brevispinosum*; (s) *Selenopemphix quanta*, and *Selenopemphix nephroides*; (t) *Quinquecuspsis concreta*; (u)

Echinidinium karaense, *Echinidinium aculeatum*, *Echinidinium granulatum*, *Echinidinium delicatum*, *Echinidinium transparentum*; **(v)** *Trinovantedinium applanatum* and *Trinovantedinium variabile*; **(w)** cyst of *Protoperidinium americanum*; **(x)** cyst of *Protoperidinium fukuyoi*; **(y)** cyst of *Polykrikos schwartzii*, *Polykrikos kofoidii*, and *Polykrikos?* sp. – Arctic type.

Figure 6. On the left, ordination diagrams of canonical correspondence analysis (CCA) axes 1 and 2; on the right, corresponding diversity diagrams or number of species. **(a)** analyses performed on all taxa; **(b)** analyses performed on the phototrophic taxa only; **(c)** analyses performed on the heterotrophic taxa only. The acronyms of taxa are the same as in Table 2 and the abbreviations of environmental parameters are the same as in Table 3. Heterotrophic taxa are indicated by solid triangles and phototrophic taxa by open triangles.

Figure 7. Distribution of the first, second and third components from canonical correspondence analysis (CCA) performed on all taxa.

Figure 8. Ordination diagram for canonical correspondence analysis (CCA) axes 1 and 2 performed showing the distribution of samples. Results are from the analyses performed with all taxa (n=71) and all samples (n=1968) as in Figure 6a. Samples from the Arctic are in green, the North Atlantic in red and the North Pacific in blue. The ellipses illustrate schematically the assemblages discussed in the text; the abbreviations correspond to the main drivers among environmental parameters: sea-ice cover (ICE), sea-surface temperature (SST) and salinity (SSS), and productivity from winter (PPw) to summer (PPsu).

LIST OF TABLES

Table 1. List of taxa in the n=371 (Rochon et al., 1999), n=1492 (de Vernal et al., 2013a) and n=1968 (this study) databases. Note that the list is not exclusive as new species and/or rare species recovered from recent sediments (Limoges et al., this issue; Mertens

et al., this issue) were not included. The acronyms in parentheses next to the taxa names indicate grouping. The acronyms in gray correspond to taxa we suggest merging or omit for statistical treatments due to rarity in the present database and/or possible equivocal identification.

Table 2. List of dinocyst taxa (n=71) and respective acronyms in the n=1968 database. Information on known trophic preference (H for heterotrophic and P for phototrophic), and occurrences (numbers and maximum percentages) are summarized. The taxa in red correspond to taxa we grouped for statistical treatments either because of excessively low occurrences or because of possible identification biases. Some other taxa also in red were not used because of unclear/overly broad taxonomic affinities or rarity (see text section 2.2).

Table 3. Weighted correlation matrix (r) of environmental parameters (17 parameters, 1968 sites).

Table 4. Summarized results of canonical correspondence analyses from analyses using **a)** the entire data set (71 taxa, 1968 sites), **b)** the data set with phototrophic taxa only (41 taxa, 1926 sites), **c)** the data set with heterotrophic taxa only (30 taxa, 1895 sites).

Table 5. Average, standard deviation (SD), and variance inflation factors (VIF) of environmental parameters

SUPPLEMENTARY MATERIAL

Figure S1a. Cross-correlation matrix of percentages of dinocyst taxa (n=71) in the n=1968 database. See Table 1 for explanation of variable codes and Table S3a for the values.

Figure S1b. Cross-correlation matrix of environmental parameters, including the monthly mean productivity and sea-ice concentration, in the n=1968 database. See Table 3 for explanation of variable codes and Table S3b for the values.

Figure S1c. Correlation matrix of percentages of dinocyst taxa (as in figure S1a) and environmental parameters (as in figure S1b) in the n=1968 database. Variable codes as in Figures S1a and S1b. See Table S3c for the values.

Table S1. Study sites for the n=1968 database: location (latitude, longitude), laboratory ID, cruise/core number, coring device, depth in the core, dinocyst count, dinocyst concentration, analyst and reference.

Table S2. Percentages of dinocyst taxa and environmental parameters in the n=1968 database.

Table S3a. Cross-correlation matrix of percentages of dinocyst taxa (n=71) in the n=1968 database.

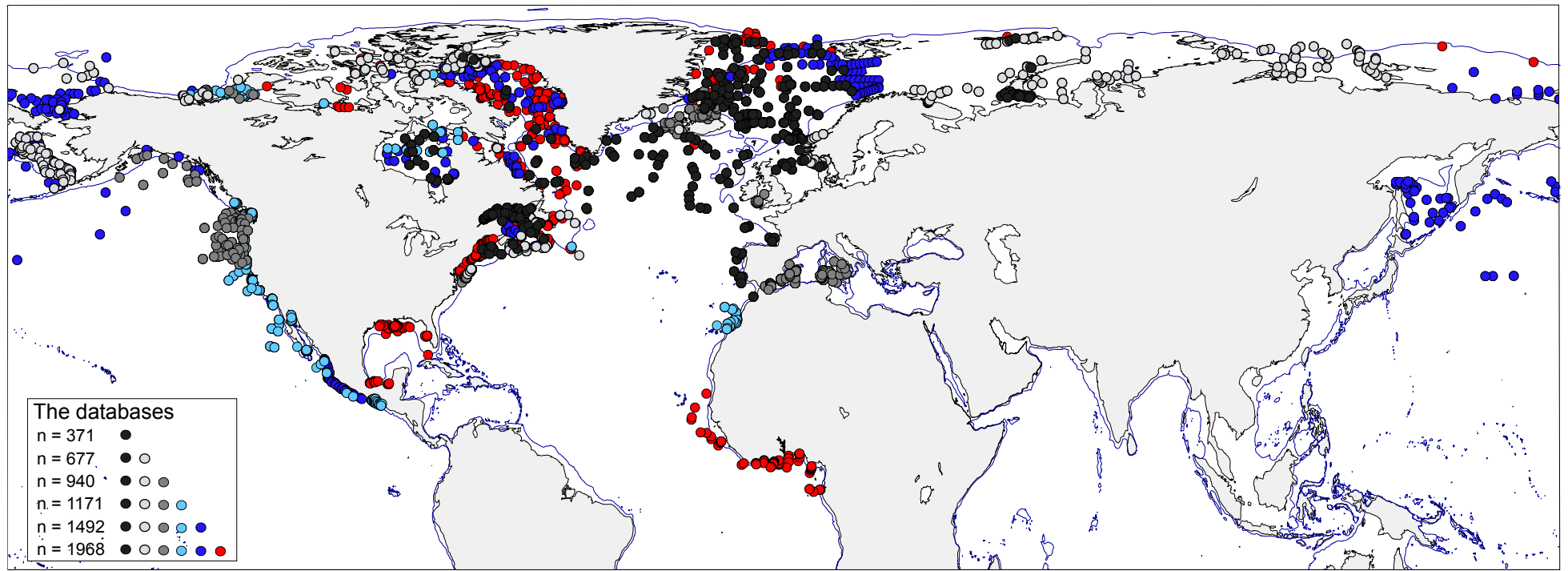
Table S3b. Cross-correlation matrix of environmental parameters, in the n=1968 database.

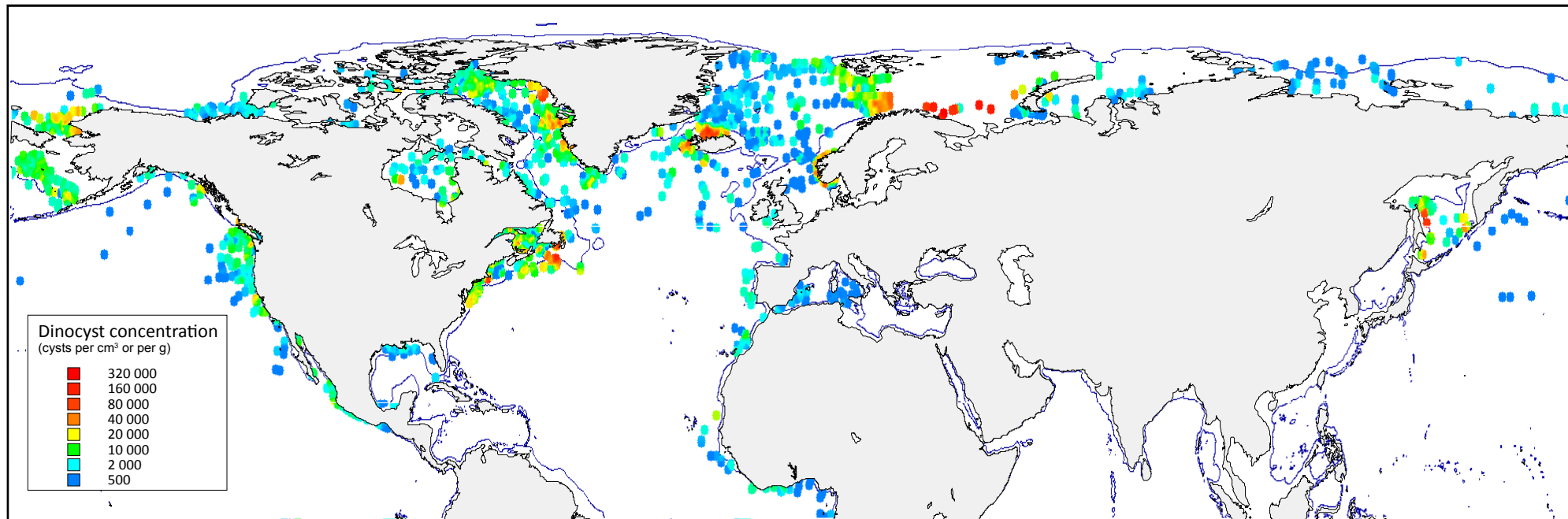
Table S3c. Correlation matrix of percentages of dinocyst taxa (as in Table S3a) and environmental parameters (as in Table S3b) in the n=1968 database.

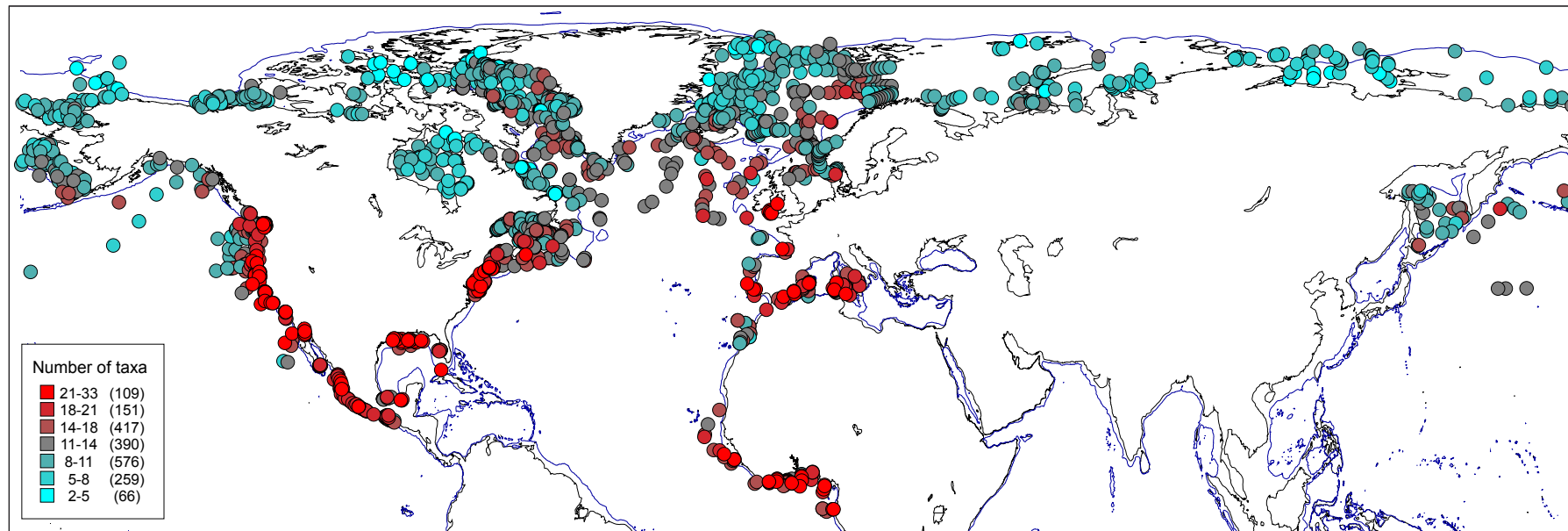
Table S4a. CCA results from the entire data base (71 taxa, 17 environmental parameters, 1968 sites).

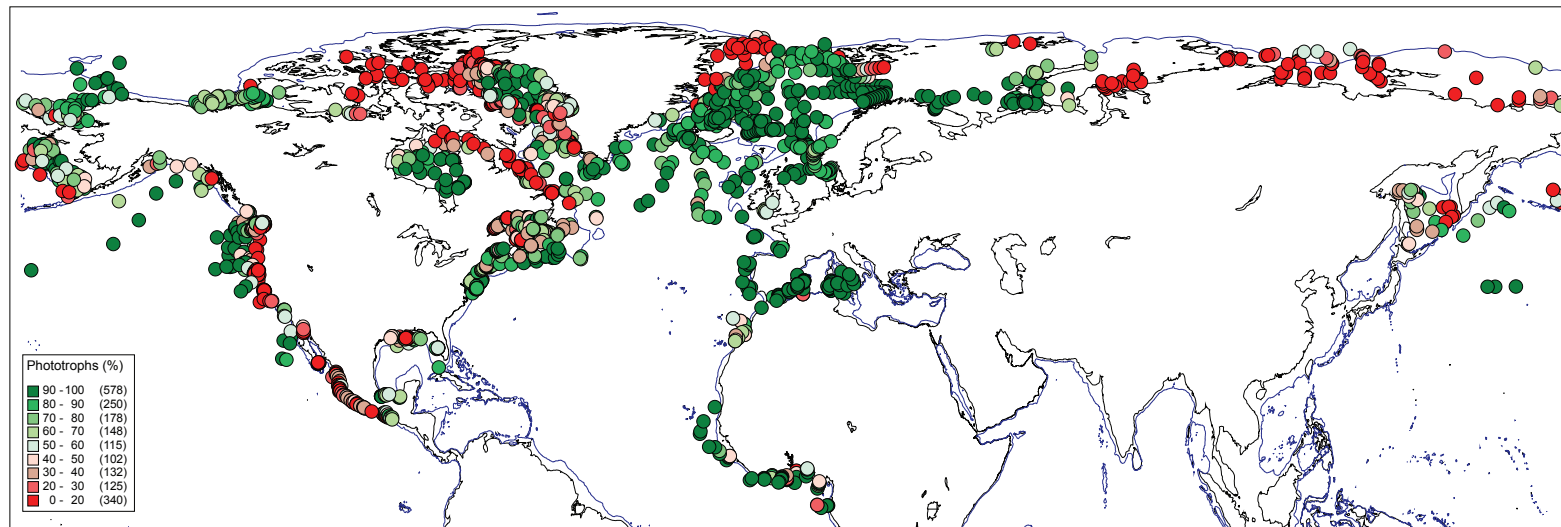
Table S4b. CCA results from the subset of data including phototrophic taxa only (41 taxa, 17 environmental parameters, 1926 sites).

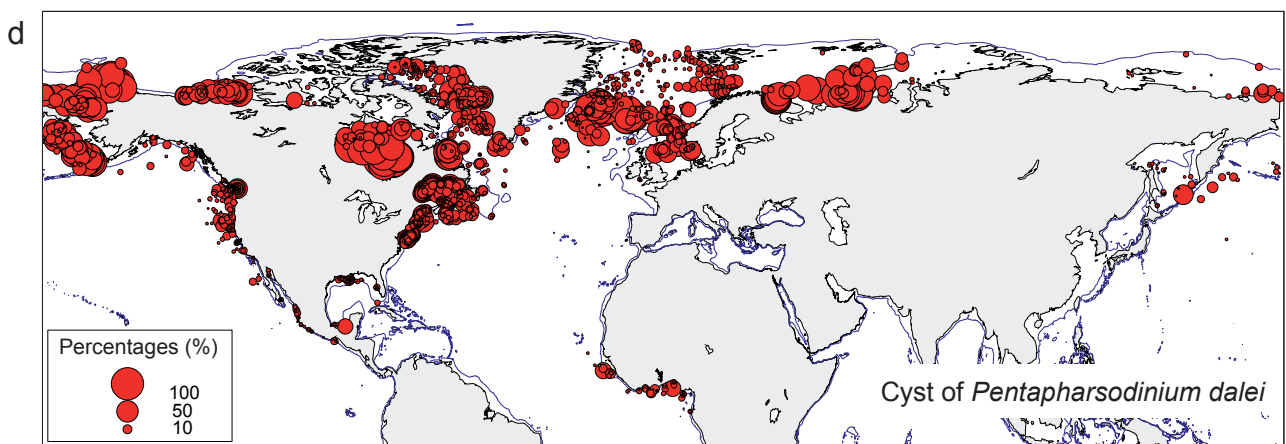
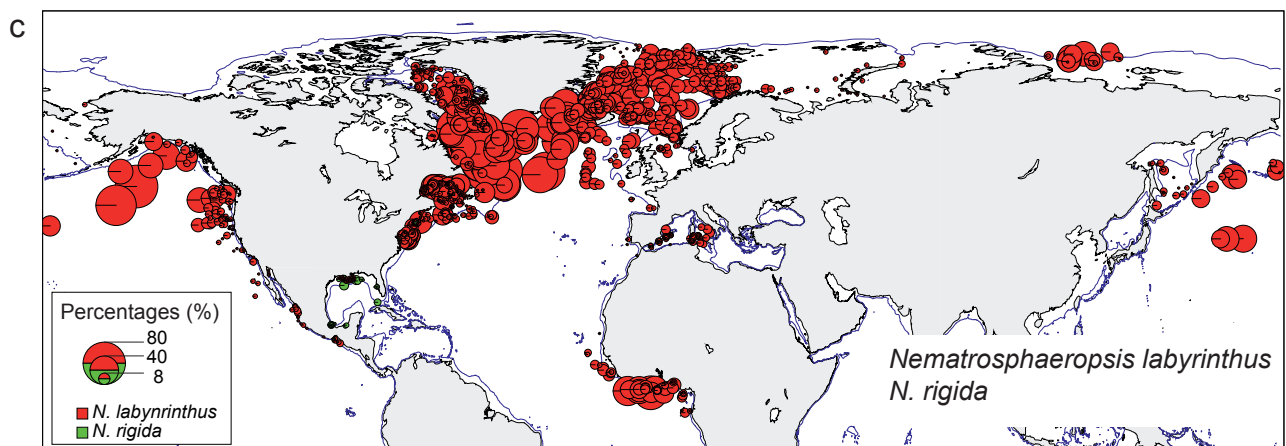
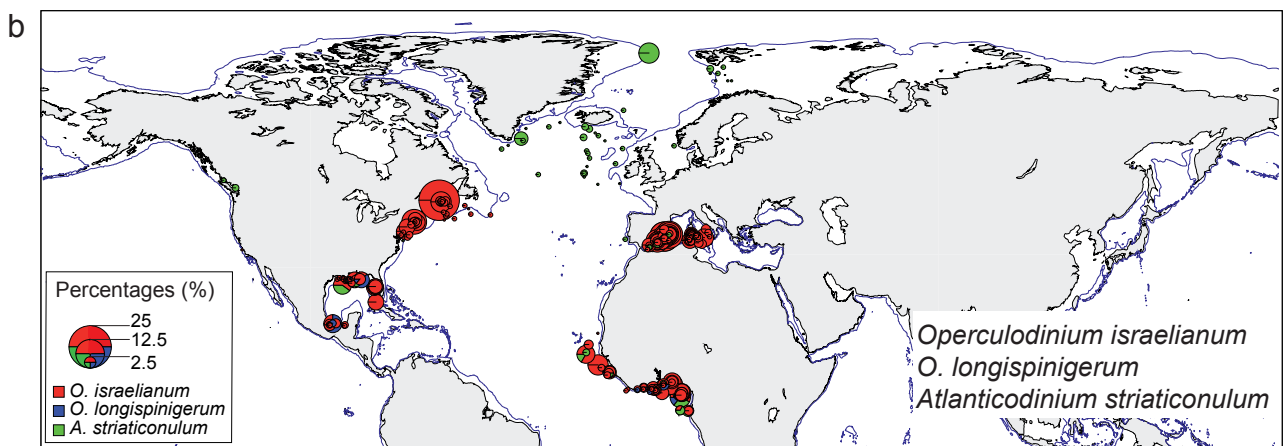
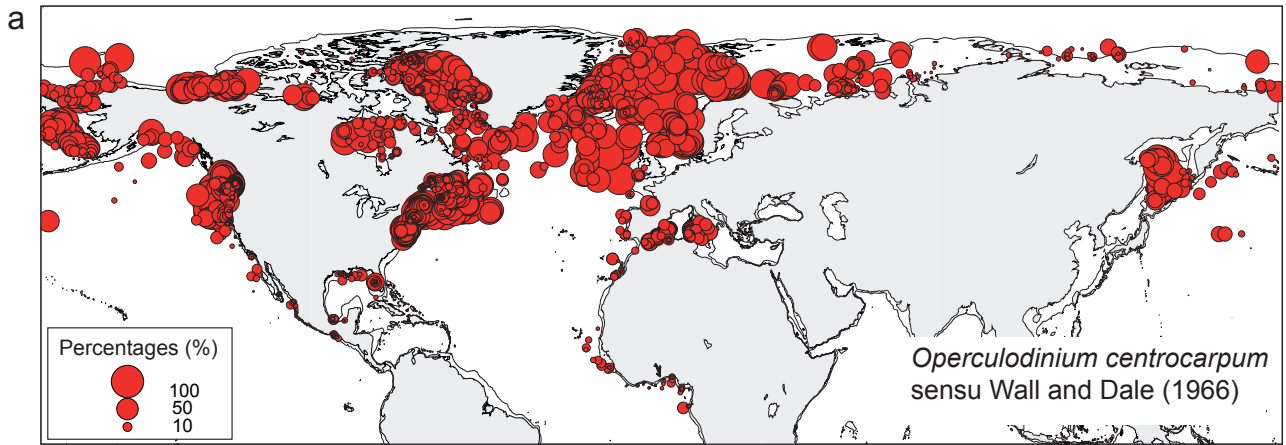
Table S4c. CCA results from the subset of data including heterotrophic taxa only (30 taxa, 17 environmental parameters, 1895 sites).

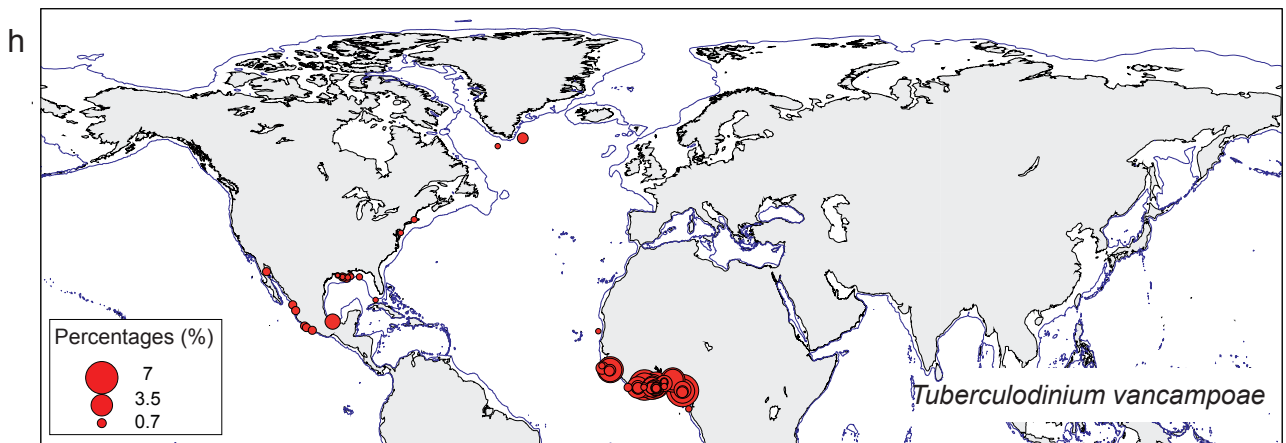
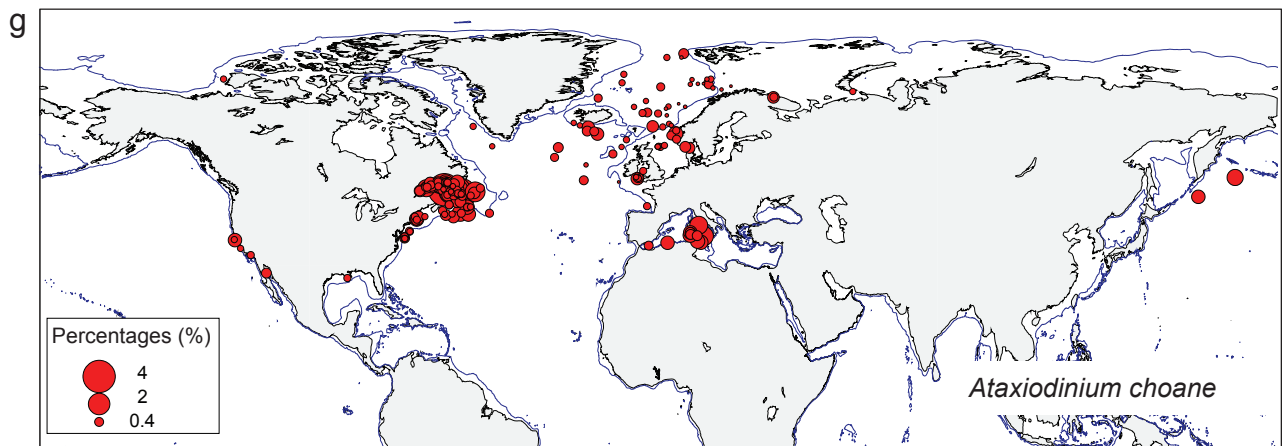
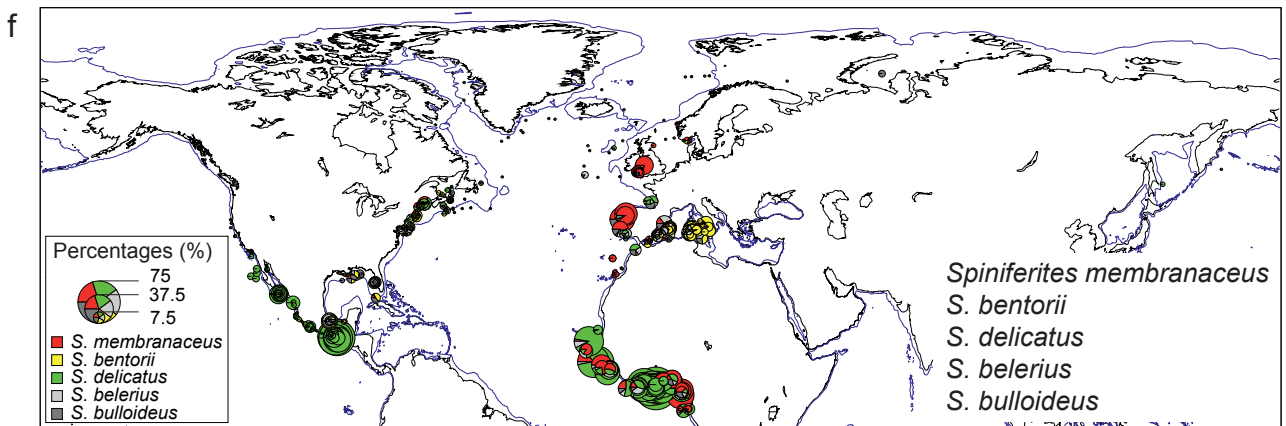
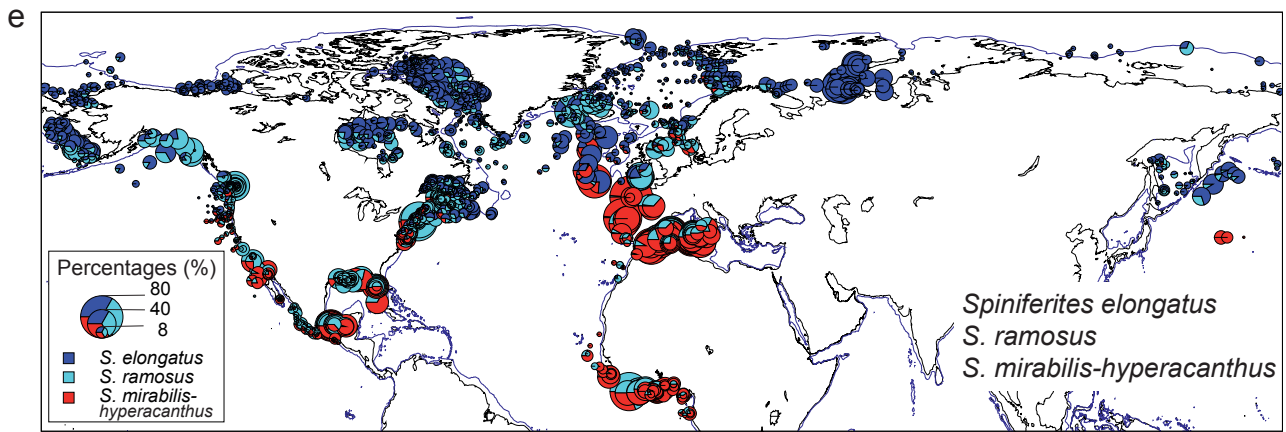




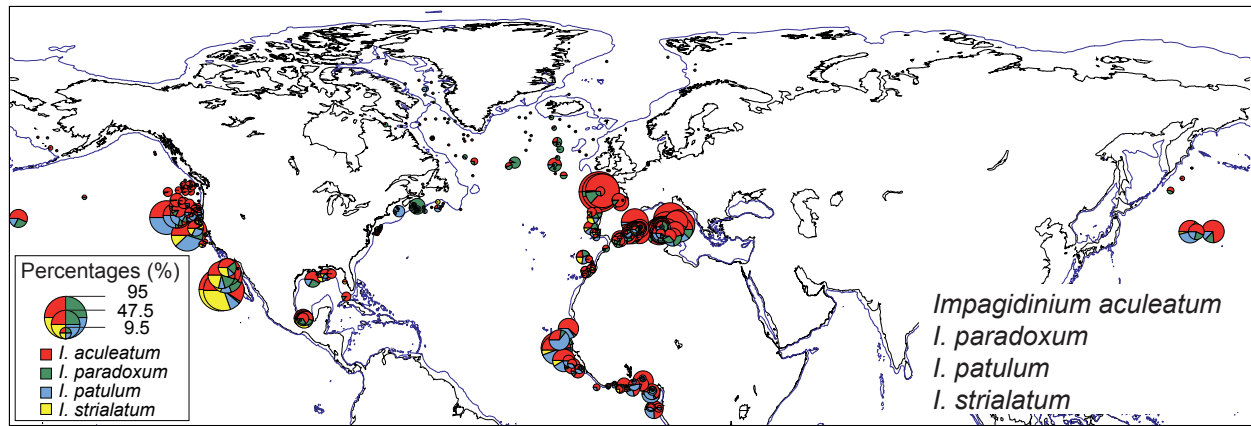




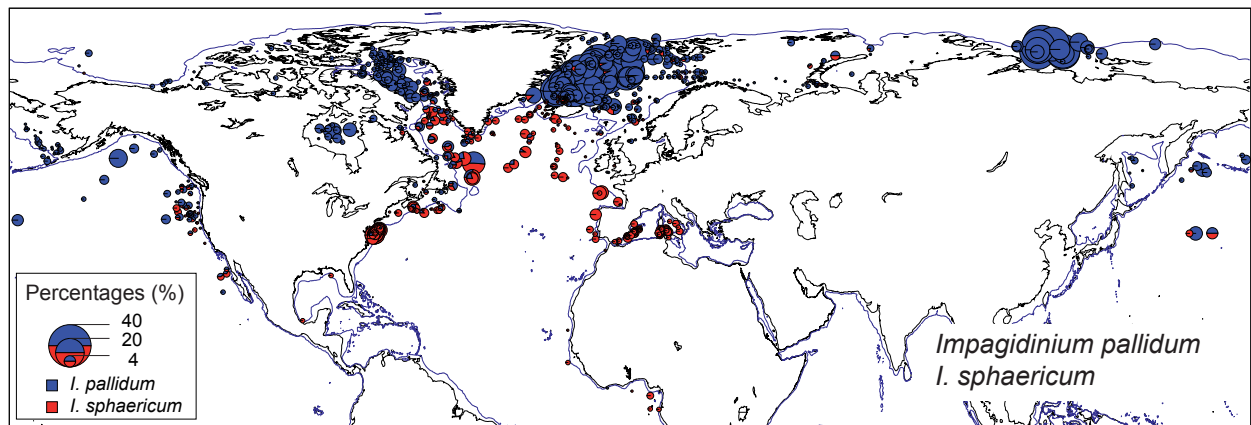




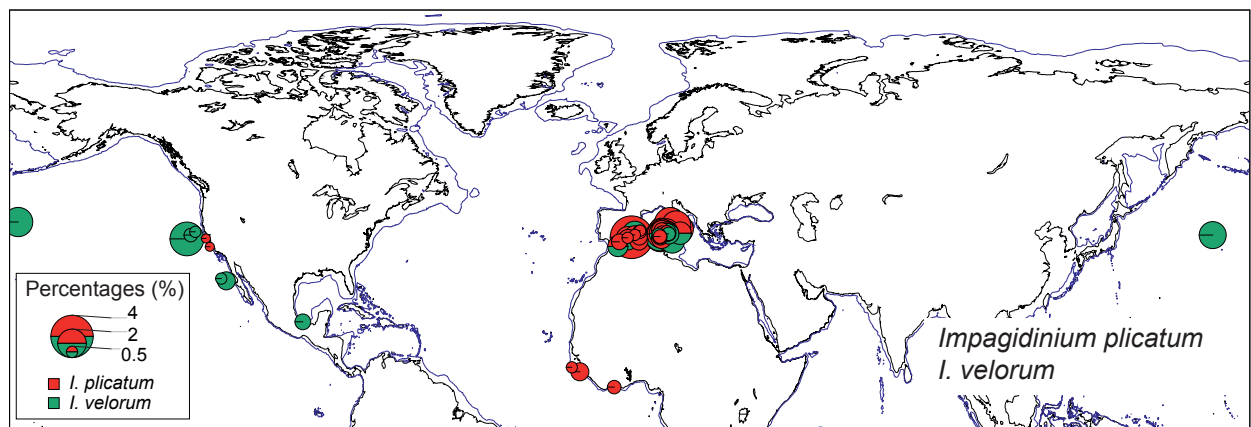
i



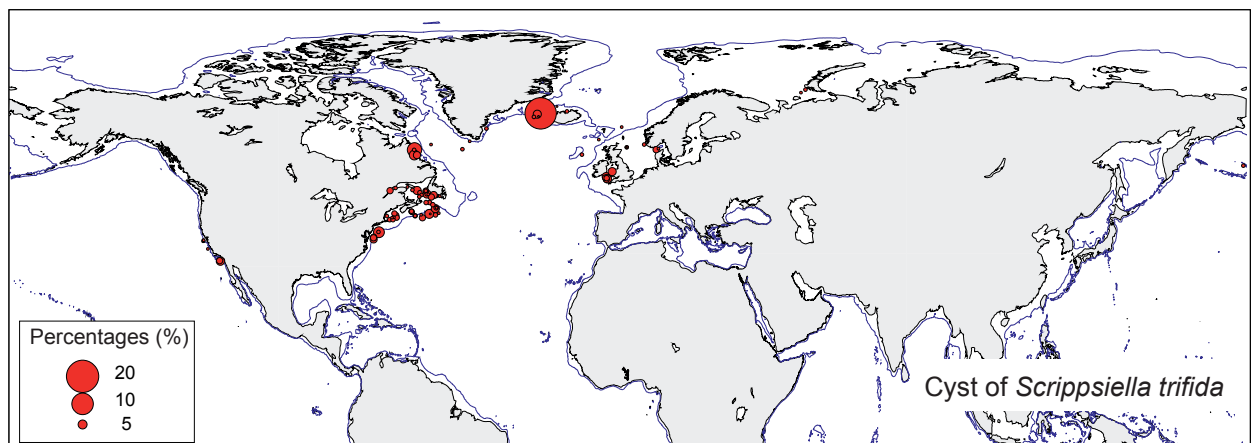
j



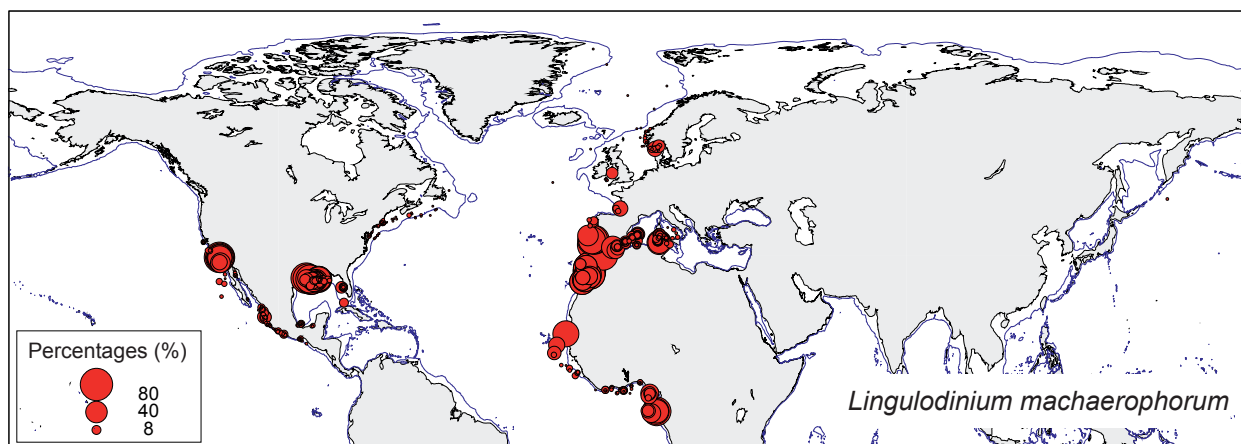
k



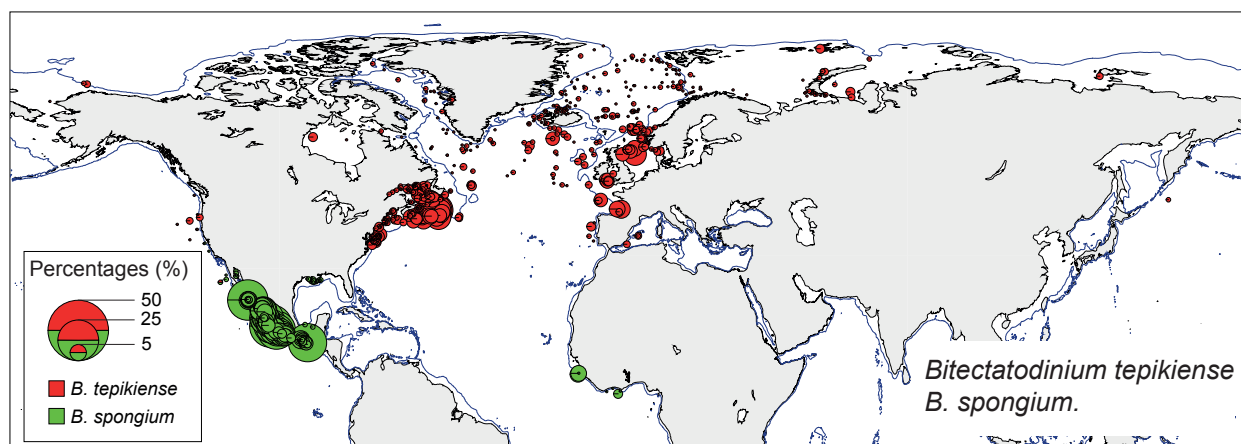
l



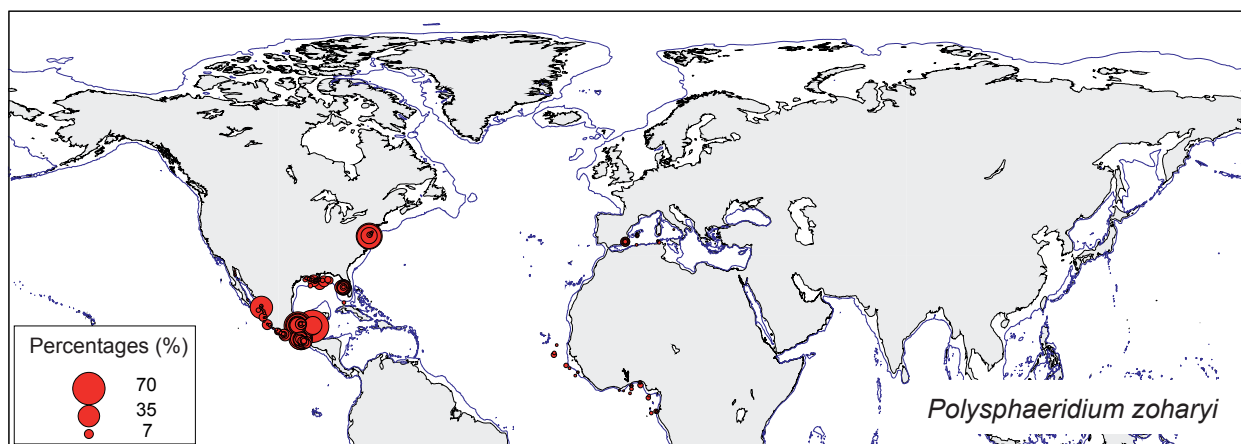
m



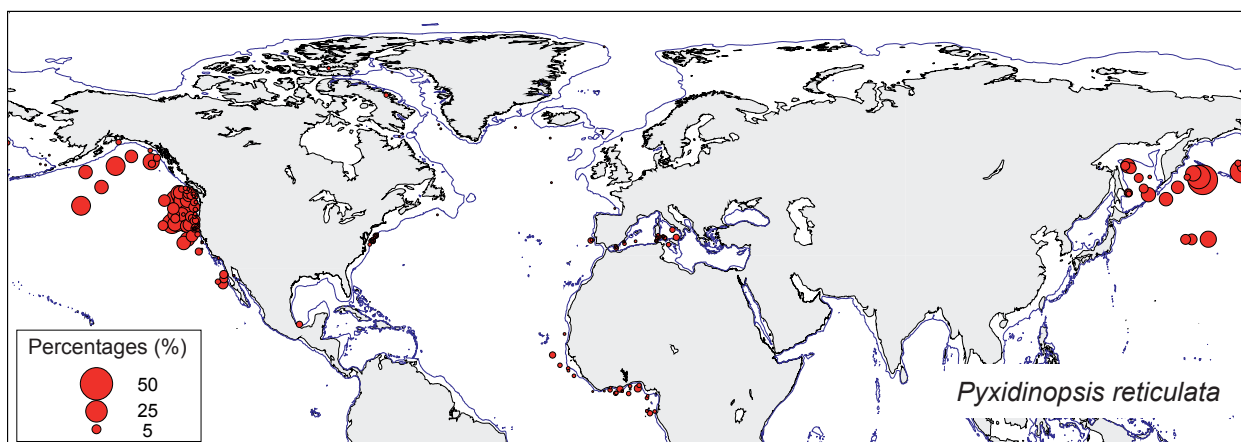
n



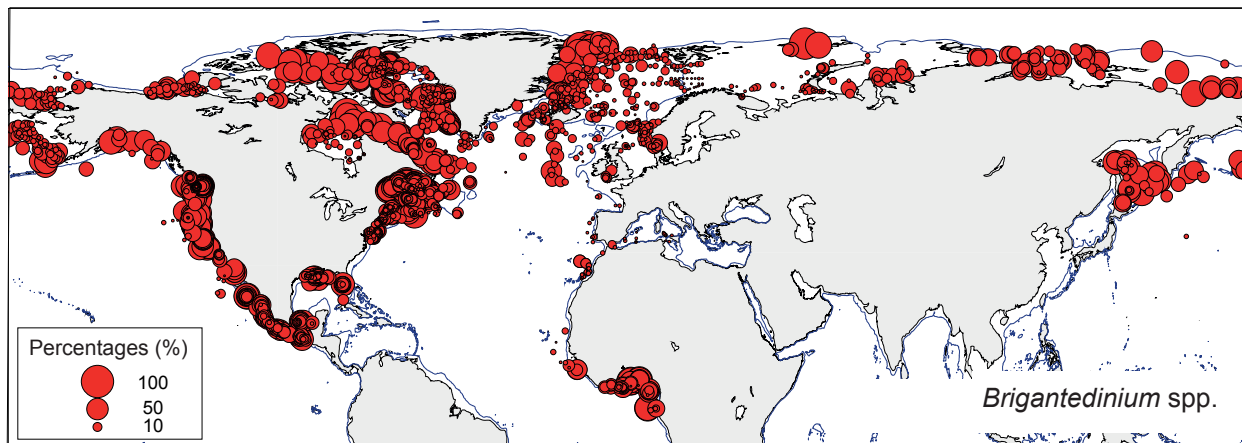
o



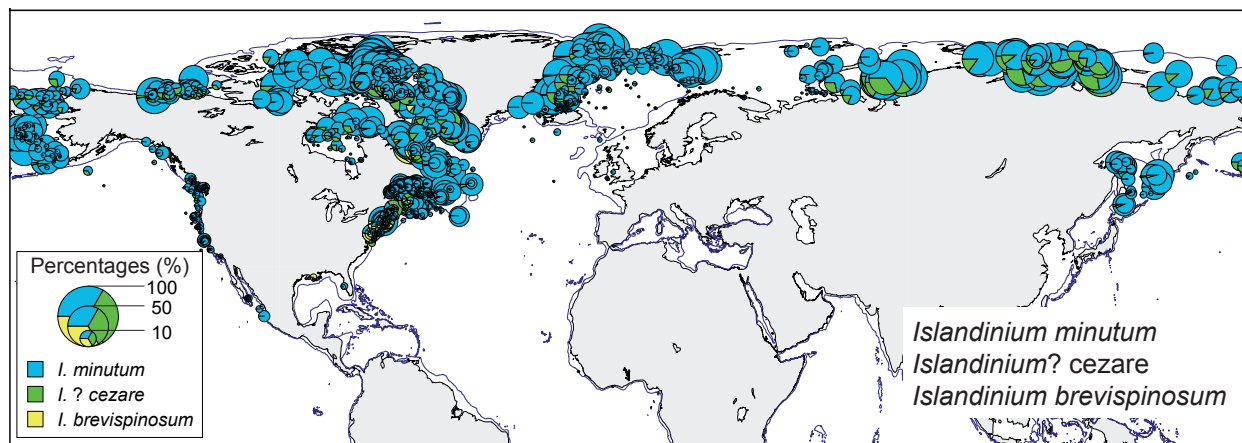
p



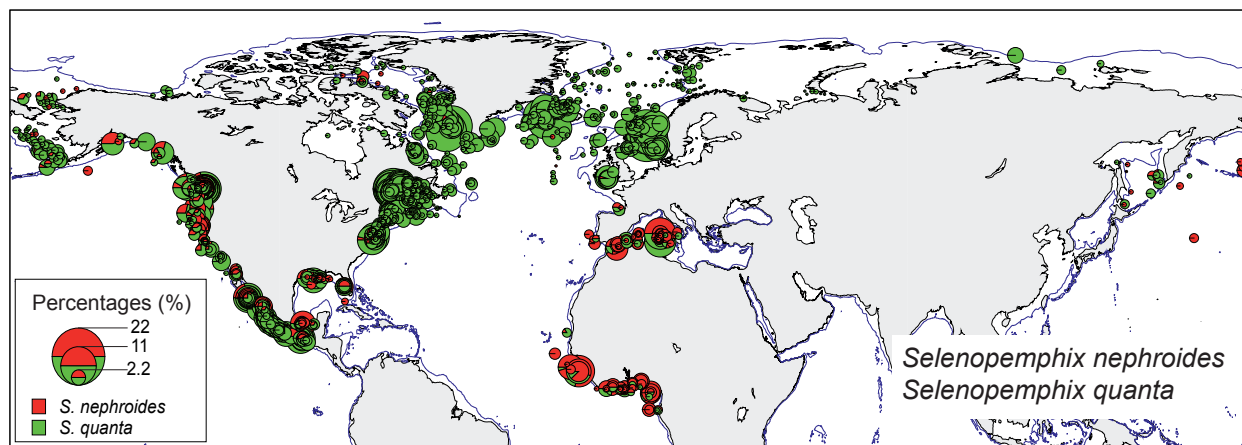
q



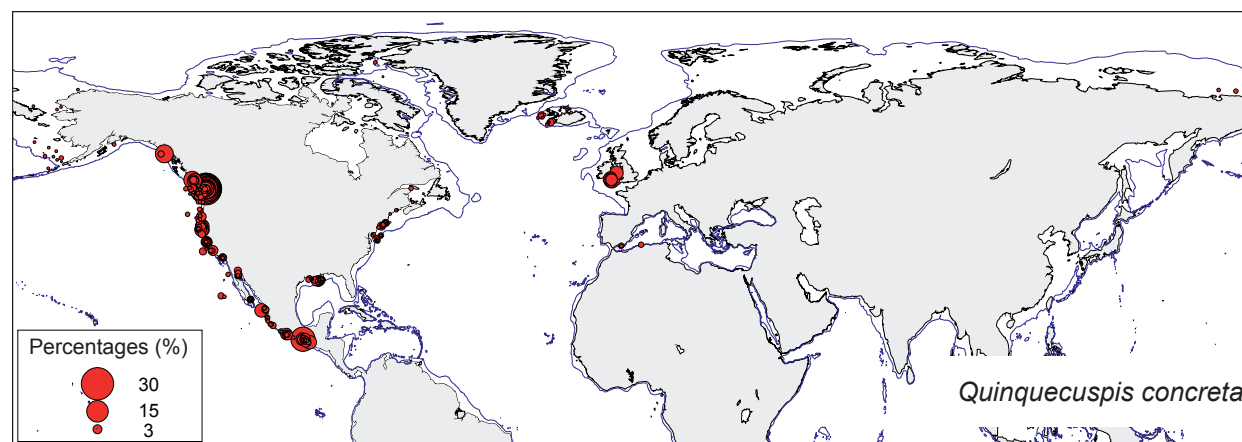
r



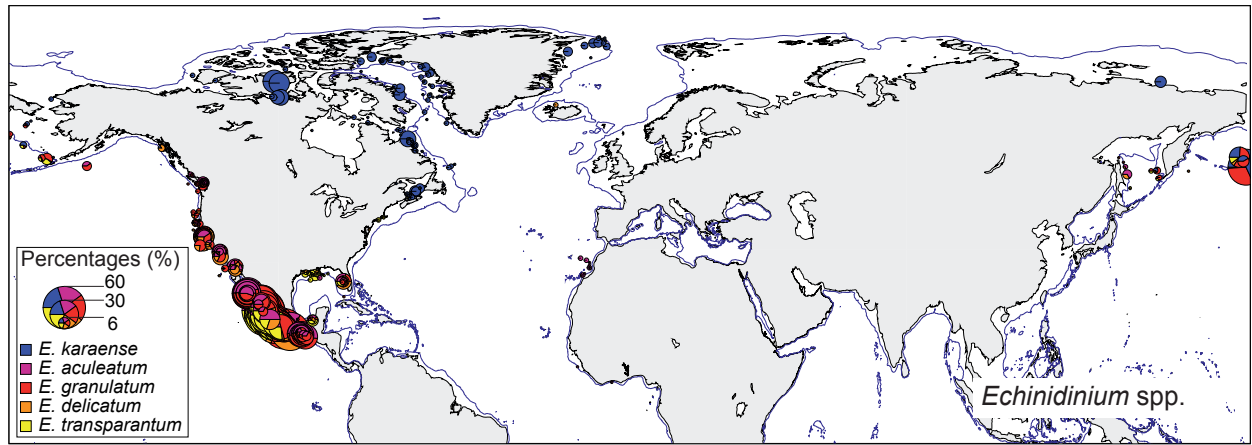
s



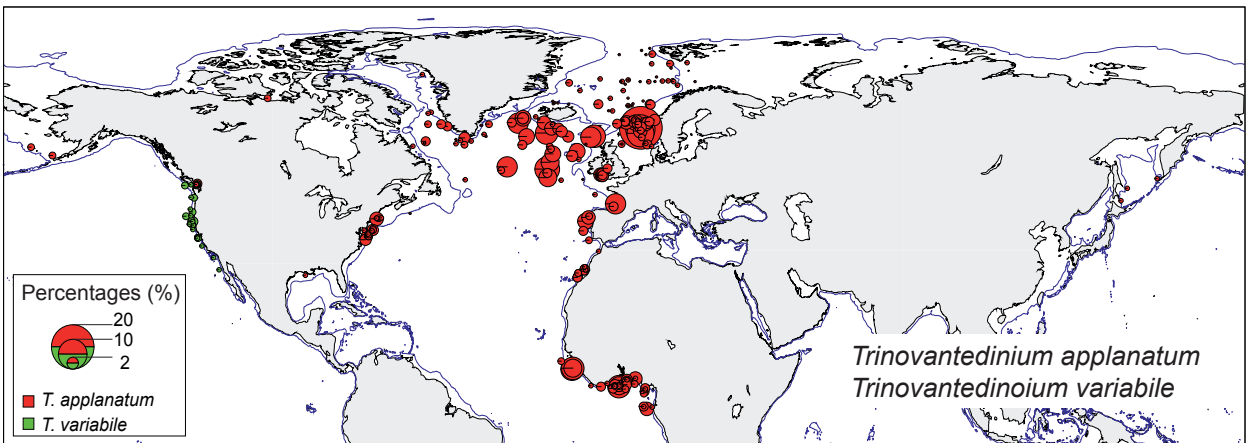
t



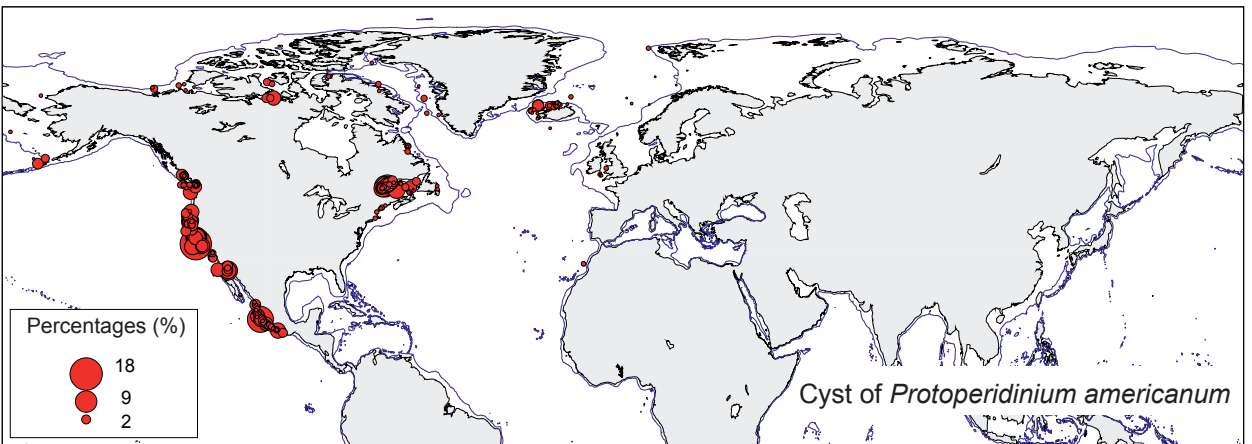
U



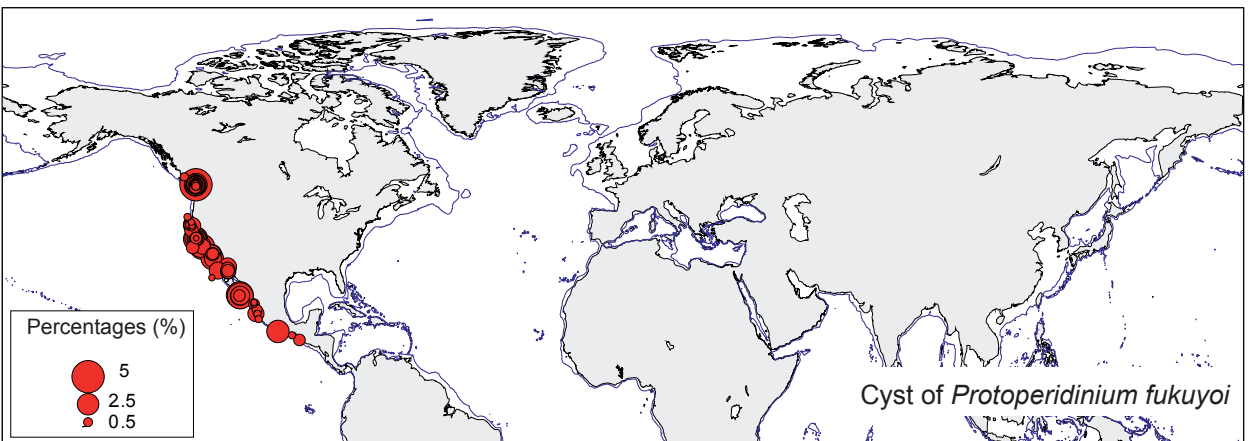
V



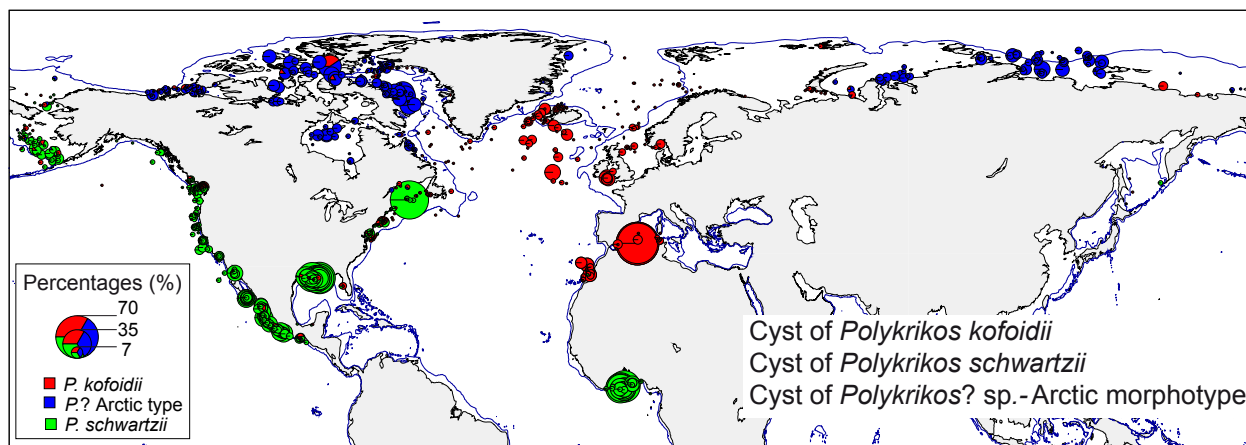
W

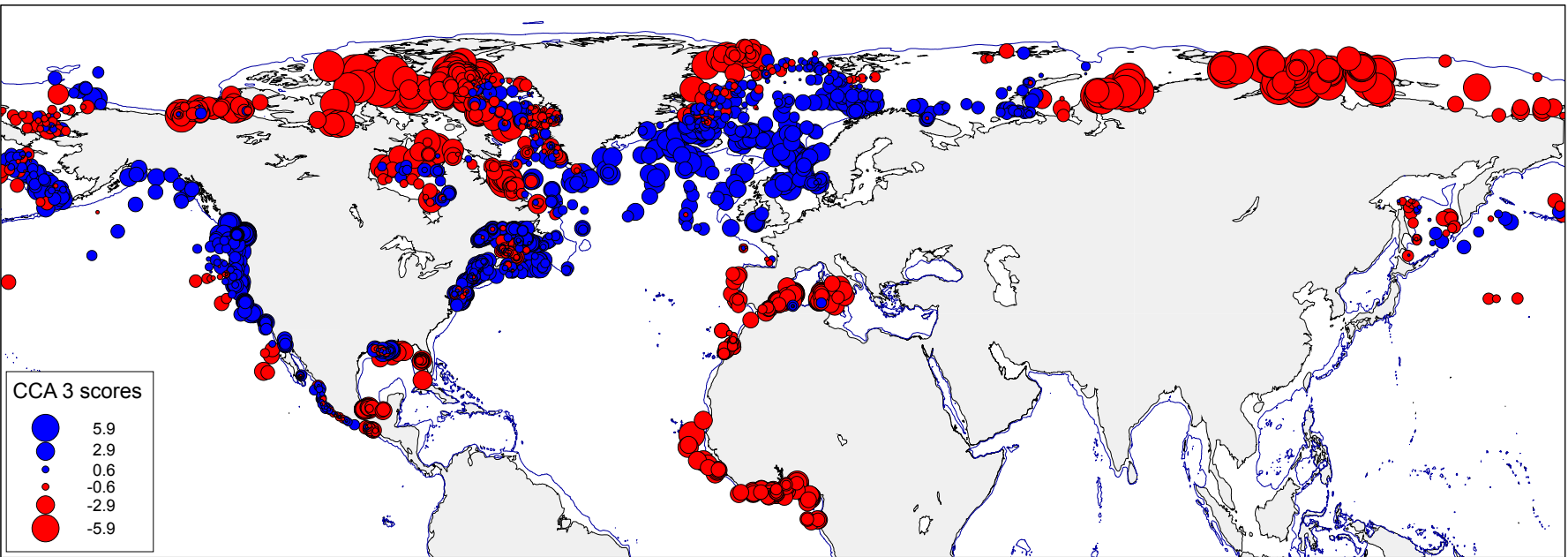
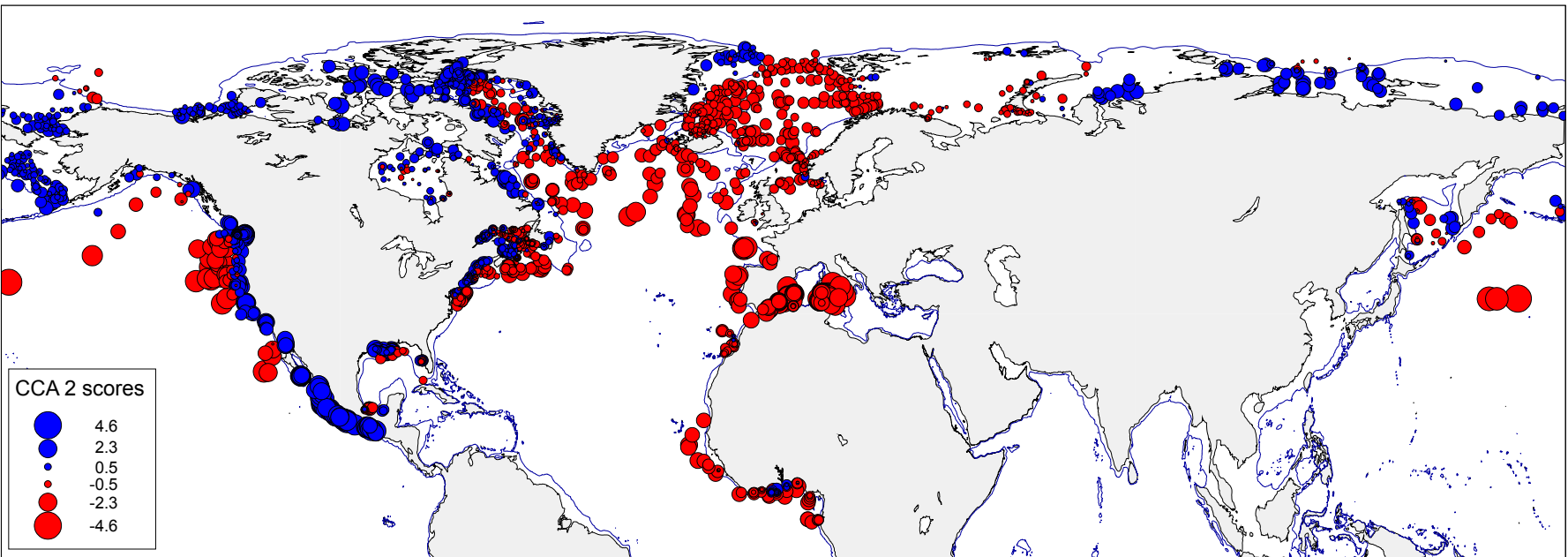
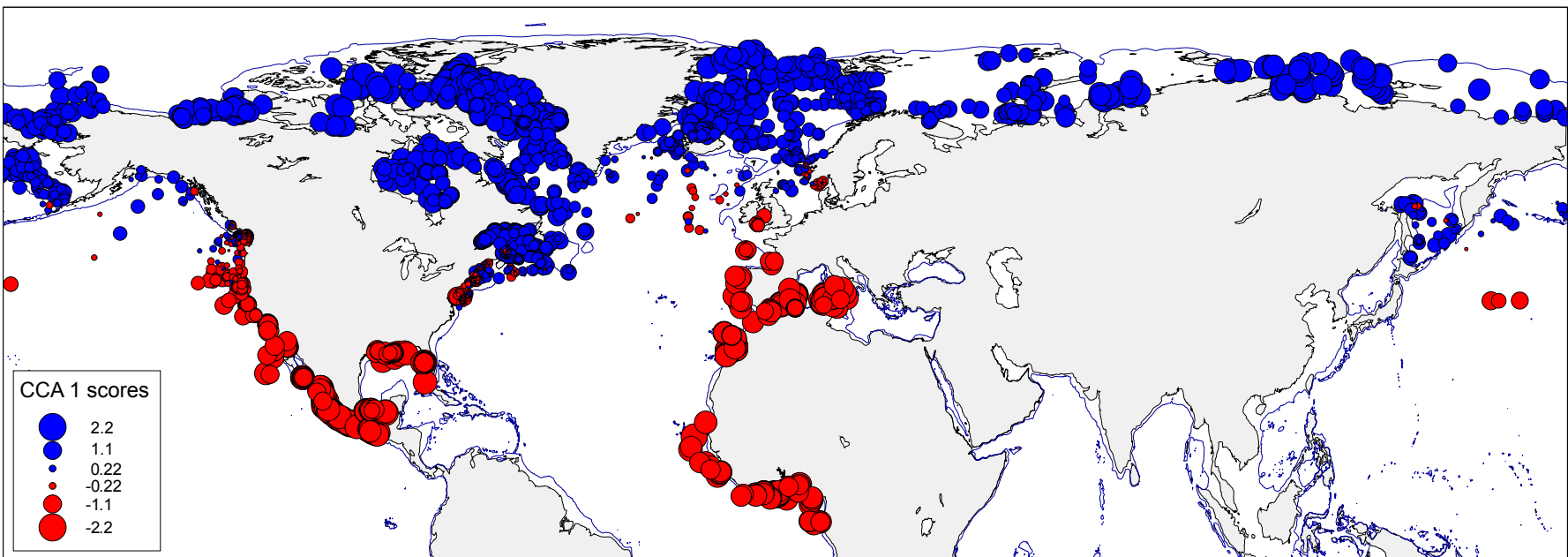


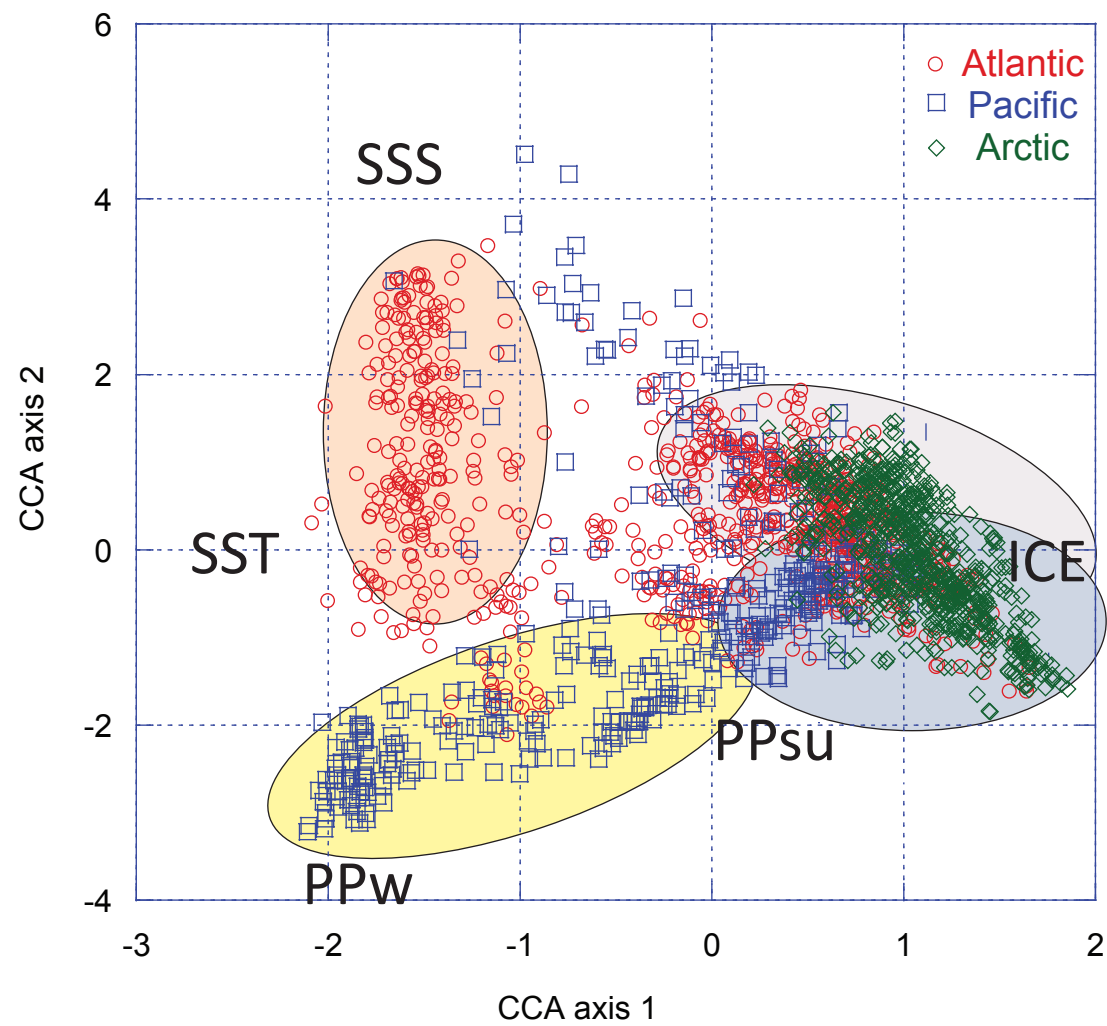
X

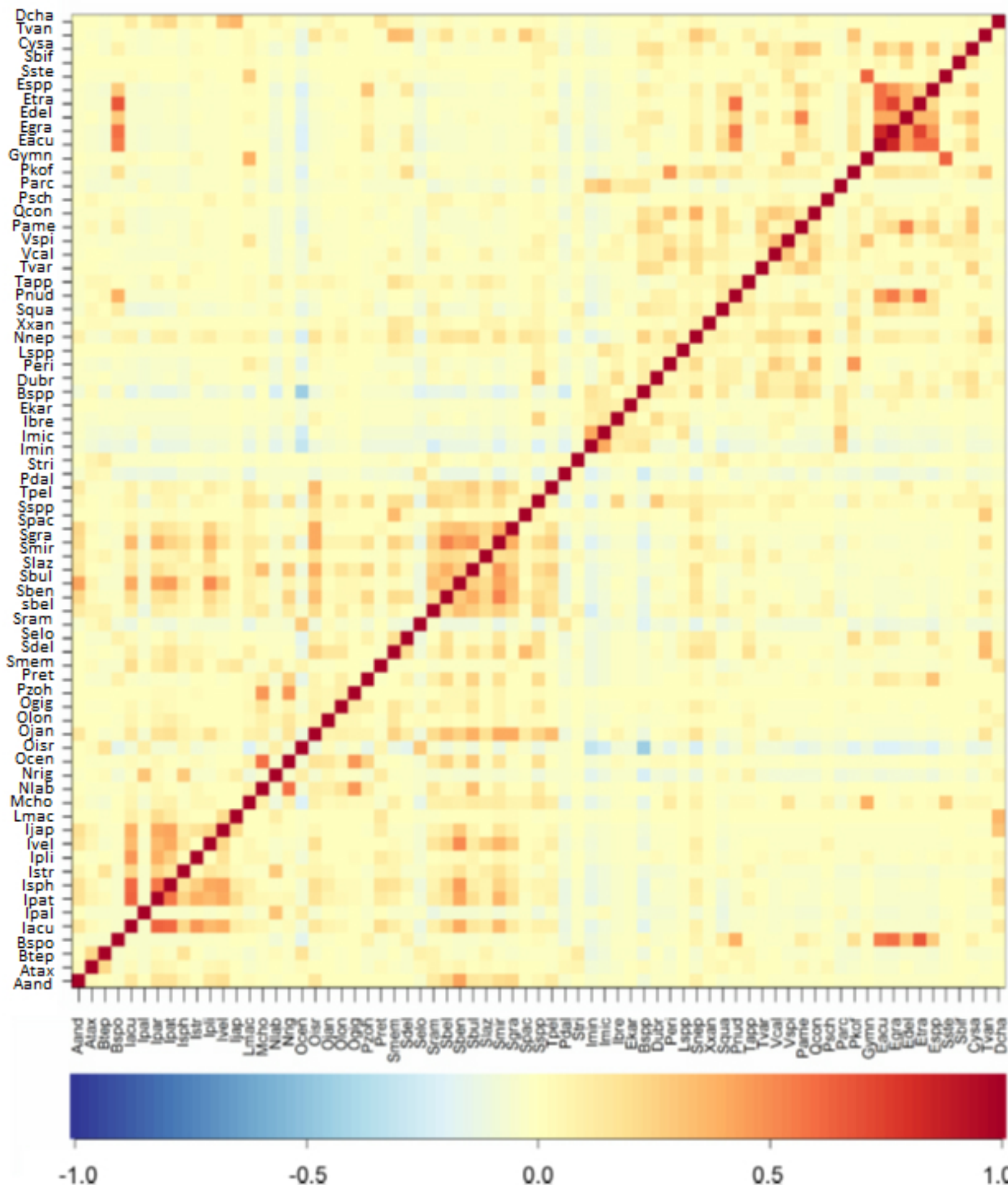


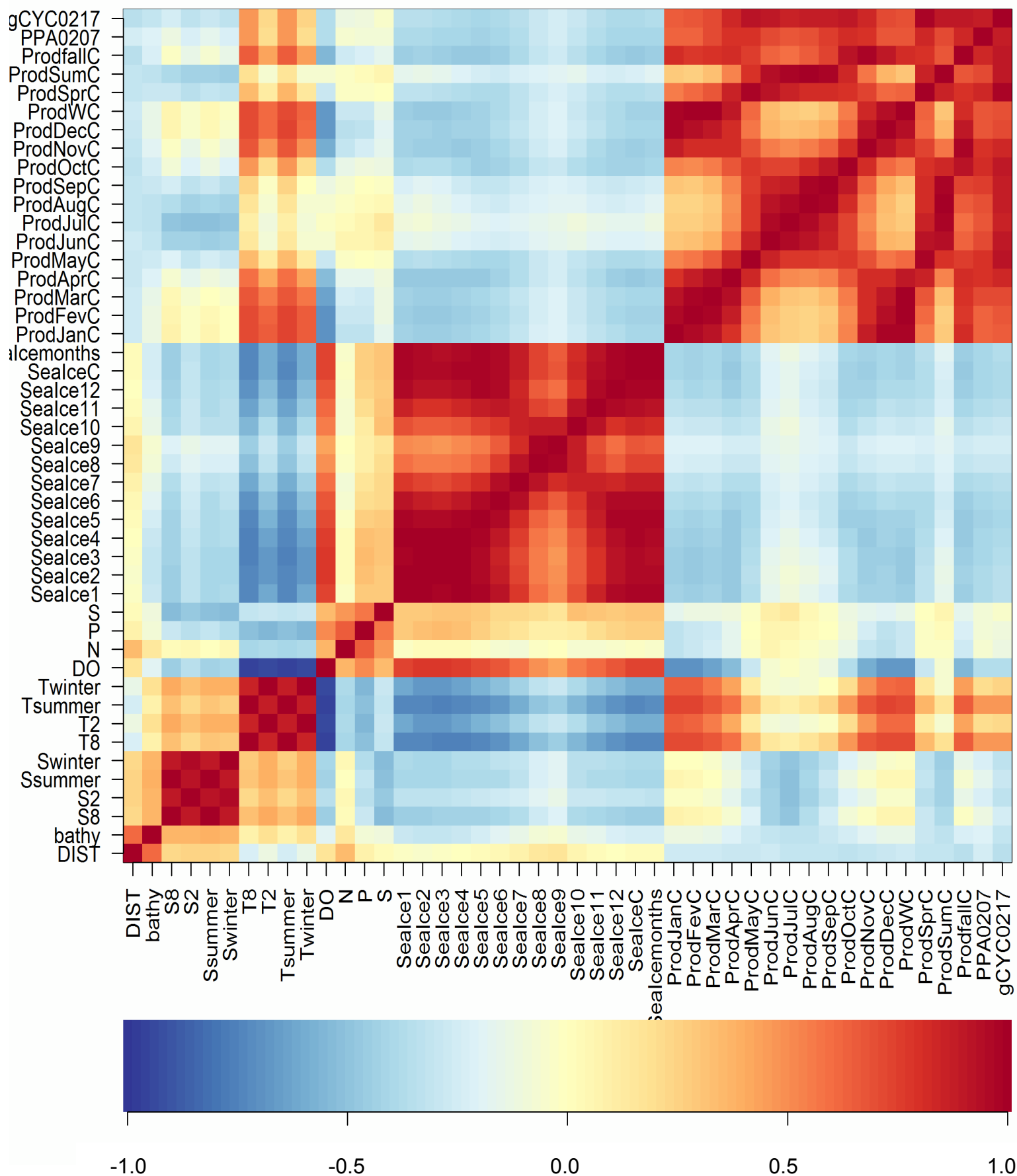
y

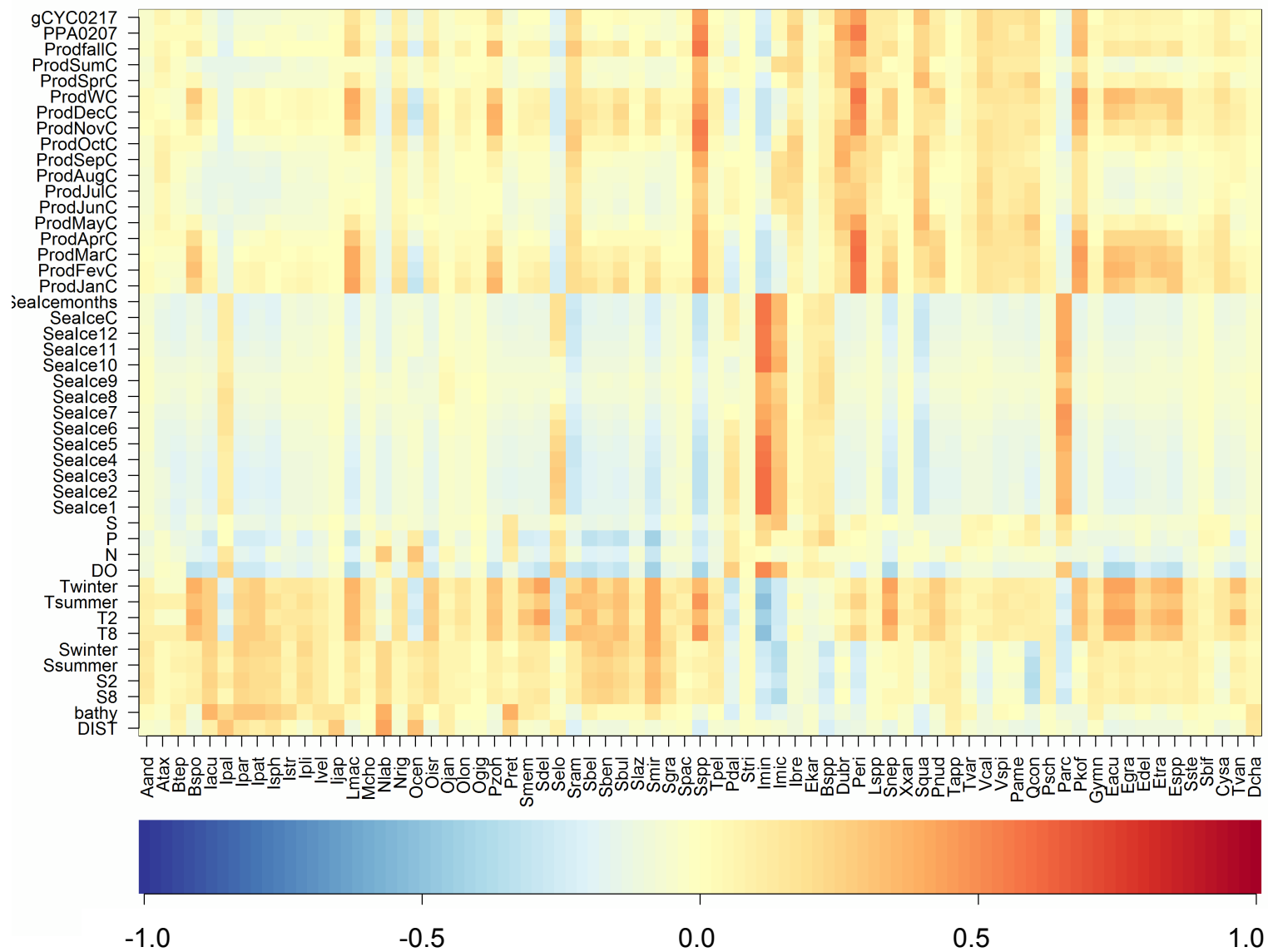












1
2
3 **Declaration of interests**
4

5 ☒ The authors declare that they have no known competing financial interests or personal relationships
6 that could have appeared to influence the work reported in this paper.
7

8
9 ☐ The authors declare the following financial interests/personal relationships which may be considered
10 as potential competing interests:
11

12
13
14
15
16
17
18
19
20

21
22
23
24 
25
26
27
28
29
30
31
32
33
34
35
36
37
38
39
40
41
42
43
44
45
46
47
48
49
50
51
52
53
54
55
56